eman ta zabal zazu

Universidad del País Vasco

Euskal Herriko Unibertsitatea

Biofunctional iron oxide nanoparticles as vaccine adjuvants for enhanced anti-cancer immunotherapy

PhD Thesis

Ana Isabel Bocanegra Gondan

2017

Table of contents

Chapter 4: Application of the complex ZnSPION-Poly(I:C)-imiquimod as an immunotherapeutic agent in a mouse model of melanoma.

Agradecimientos

En primer lugar, mi agradecimiento a mi director de tesis, Juan C. Mareque Rivas, por darme la oportunidad de comenzar esta aventura y de llegar hasta el final.

También quiero expresar mi gratitud hacia todos los compañeros de CIC biomaGUNE que me acompañaron en el camino tanto en los momentos buenos como en los más duros. Me llevo de cada uno de vosotros los recuerdos de los mejores momentos de risas, complicidad, excursiones, etc, que nunca olvidaré. No obstante, tengo que hacer una mención especial con el mayor cariño a Aintzane; nunca tendré palabras suficientes para agradecer tanta ayuda, tanto apoyo y tanto cuanto aprendí de ti. Desde el primer día hasta el último con una sonrisa y siempre con una palabra de aliento preparada, siempre con la mayor disposición a ayudar. Sin duda has marcado un antes y un después y sin ti no habría sido posible llegar hasta el final. Por esto y mucho más te debo un reconocimiento muy especial. Tampoco puedo dejar de dar un agradecimiento especial a Nina, quien ha sido para mí un pilar esencial dentro y fuera del laboratorio, y a todos los miembros de las plataformas de CIC biomaGUNE y, muy especialmente, al personal de animalario: Clara, Sergio, Ainhoa y Ander, por vuestra infinita ayuda, apoyo, paciencia y por el cariño que me habéis transmitido durante todos estos años. A todos vosotros, os deseo lo mejor.

Ya han pasado años, pero con vosotros empecé este camino y os tengo siempre presentes, por eso aprovecho esta oportunidad para agradecer a los que fueron mis compañeros en CABIMER: Mario, Pablo, Curro, Elena, Ali, Tati… Vosotros me enseñásteis lo que significa realmente ser buenos compañeros y ojalá algún día vuelva a encontrar un ambiente de trabajo tan bueno como el que compartí con vosotros. Os doy las gracias de corazón por todo lo que me enseñásteis y, sobre todo, por vuestra amistad.

Quisiera también expresar mi cariño y gratitud hacia todas las personas que me han acompañado a lo largo de esta andadura fuera del laboratorio. Por una parte, a los compañeros de pista de bádminton (y de pintxos), Ágata, Manu, Linda, Lucie, Sonia y Julio; al equipo de corredoras de biomaGUNE, María, Bea, Susana y Ruta; a los que han sido mis estupendos

compañeros de piso, Danielle, Goretti, Denis, Cyrille y Cristina; y a los amigos que habéis ido apareciendo para quedaros, Germán, Kepa, Álvaro y Thuy, Izaskun y Álvaro (II), Geraldine, Violeta, Gurutze y Guillermo. Gracias a todos por haber hecho de estos cuatro años una experiencia inolvidable, por haber compartido tantos buenos momentos y por todo el apoyo y cariño que me habéis dado.

Gracias de una manera muy especial a Enrique, mi compañero del camino, mi amigo, mi amor. Tú has sido mi sostén, mi inspiración, mi motor para seguir y seguir adelante. Has sido el mayor apoyo en los momentos difíciles y el mejor compañero en los momentos felices. El espejo en el que poder mirarme. Sin ti no habría podido llegar hasta aquí. Por todo, gracias de corazón. Y que nos quede aún mucho por recorrer, juntos. Gracias también a mi segunda familia, que generosamente me han acogido con los brazos abiertos, y a los sobrinos prestados que me han llamado tía por primera vez.

Quiero recordar también a mis amigos, a los de siempre y a los de casi siempre. Bea, Irene, Raquel, Fran, Andrea, Choni, Inma, Paula, Dolo, y los del manicomio, Lydia, Valme y Alberto. Estar con vosotros, sea donde sea, es estar en casa. Por más tiempo que pase sé que siempre estaréis ahí. Os agradezco de corazón vuestra amistad, que seguro continuará por muchos años más.

Por último, el agradecimiento más importante a mi familia, a mis padres y a mi hermano. Gracias por haberme enseñado a ser todo lo que soy, por los valores que me habéis inculcado, por haberme dado siempre cuanto he necesitado hasta sin poder y de la manera más generosa y amorosa, sin esperar nada a cambio. Gracias por haber estado y estar siempre dispuestos para ayudarme en todo. Os quiero.

Y gracias a ti, papá, que aún sigues desde el cielo empujándome día tras día a seguir adelante. Ojalá hubieras podido llegar a leer esto, pero no pudiste ganar la batalla. Por difícil que sea de comprender y de asimilar, te has ido demasiado pronto, pero ahora estás en ese lugar donde ya no hay más dolor, donde no hay más sufrimiento. Te dedico a ti este trabajo, y a todos aquéllos que siguen en esta lucha miserable, con la esperanza y el convencimiento de que la investigación, algún día, atajará semejante sinsentido.

Abbreviations

ADCP	*Antibody-dependent cellular phagocytosis*
AEP	*Asparagine endopeptidases*
APC	*Antigen presenting cell*
BMDC	*Bone marrow derived dendritic cells*
CART	*Chimeric antigen receptor therapy*
CCR7	*C-C chemokine receptor 7*
cDNA	*Complementary DNA*
CLR	*C-type lectin receptors*
CT	*Chemotherapy*
CTL	*Cytotoxic T lymphocytes*
DAMP	*Damage associated molecular patterns*
DC	*Dendritic cell*
DD	*Death domain*
DLS	*Dynamic light scattering*
DMSA	*Dimercaptosuccinic acid*
DOTAP	*1,2-dipalmitoyl-3-trimethylammonium-propane*
dsRNA	*Double-stranded RNA*
EBV	*Epstein-Barr virus*
EDC	*1-Ethyl-3-(3-dimethylaminopropyl)-carbodiimide*
EMA	*European Medicines Agency*
EPR	*Enhanced permeability and retention*
FDA	*US Food and Drug Administration*
GM-CSF	*Granulocyte macrophage colony-stimulating factor*
g-PGA	*Poly(g-glutamic acid)*
HBV	*Hepatitis B virus*
HCV	*Hepatitis C virus*
HDAC	*Hystone deacetylases*
HLA	*Human leukocyte antigen*
HPV	*Human papillomavirus*
ICB	*Immune checkpoint blockade*
ICP-AES	*Atomic emission spectrometry*
IDO	*Indoleamine 2, 3-dioxygenase*
IFN	*Interferon*
ILC	*Innate lymphoid cells*
IONP	*Iron oxide nanoparticles*
LN	*Lymph node*

LPS	*Lipopolysaccharide*
LRR	*Leucine rich repeats*
MDA-5	*Melanoma differentiation-associated protein 5*
MDSC	*Myeloid derived suppressor cell*
MHC	*Major histocompatibility complex*
miRNA	*Micro RNA*
MNP	*Magnetic nanoparticles*
MPLA	*Monophosphoryl lipid A*
MRI	*Magnetic resonance imaging*
M_S	*Saturation magnetization*
MTT	*3-(4,5-dimethylthiazol-2-yl)-2,5-diphenyltetrazolium bromide*
MVP	M*ajor vault protein*
NHS	*N-hydroxysulfoxuccinimide*
NK	*Natural killer*
NLR	*NOD-like receptors*
NO	*Nitric oxide*
O_h	*Octahedral*
OVA	*Ovalbumin*
PAMP	*Pathogen-associated molecular patterns*
pDC	*Plasmacytoid dendritic cells*
PDI	*Polydispersity index*
PEG	*Polyethylene glycol*
PEI	*Polyethylenimine*
PET	*Positron emission tomography*
PIAS	*Protein inhibitors of activated STATs*
PLG	*Poly(D,L-lactide-co-glycolide)*
PLGA	*Poly(D,L-lactic-coglycolic acid)*
Poly(I:C)	*Polyinosinic : polycytidylic acid*
PRR	*Pattern recognition receptor*
PVA	*Polyvinyl alcohol*
R837	I*miquimod*
RES	*Reticuloendothelial system*
RLR	*Retinoic acid I (RIG-I)-like receptors*
ROS	*Reactive oxygen species*
RT	*Radiotherapy*
siRNA	*Small interfering RNA*
SOCS	S*uppressors of cytokine signaling*
SPECT	S*ingle-photon emission computed tomography*
SPION	*Superparamagnetic iron oxide nanoparticle*
SQUID	*Superconducting quantum interference device*

ssRNA	*Single-stranded RNA*
STAT	*Signal transducers and activators of transcription*
STING	*Stimulator of interferon genes*
TAA	*Tumor associated antigen*
TAM	*Tumor associated macrophages*
T_{cm}	*T central memory*
TCR	*T cell receptor*
T_d	*Tetrahedral*
T_{em}	*T effector memory*
TEM	*Transmission electron microscopy*
TGA	*Thermogravimetric analysis*
TGFβ	*Transforming growth factor β*
TIL	*Tumor infiltrating lymphocytes*
TIR	*C-terminal Toll/IL-1 receptor*
TLR	*Toll-like receptor*
TLRa	*TLR agonist*
TNFα	*Tumor necrosis factor α*
TRAIL	*TNF-related apoptosis inducing ligand*
T_{reg}	*T regulatory lymphocytes*
USPIO	*Ultra-small superparamagnetic iron oxides*
UV	U*ltraviolet*
UVB	*Ultraviolet B*
VLP	*Virus-like particle*
XPS	*X-ray photoelectron spectroscopy*
ZnSPION	*Zn^{+2} doped superparamagnetic iron oxide nanoparticle*

Resumen

El abordaje del tratamiento de una enfermedad tan compleja como el cáncer representa, en muchos aspectos, un gran desafío. A pesar de la enorme inversión en esfuerzo y capital en la investigación contra el cáncer en las últimas décadas, esta enfermedad continúa siendo hoy en día una de las principales causas de mortalidad en el mundo desarrollado. Y aún más, las previsiones indican que la incidencia de esta enfermedad continuará aumentando en el futuro, y particularmente en el caso del melanoma la tendencia indica una creciente prevalencia entre la población más joven (< 30 años).

Las terapias tradicionales se han basado principalmente en la resección quirúrgica de los tumores, quimioterapia y radioterapia. No obstante, las principales limitaciones de estas terapias residen en la falta de universalidad en la respuesta de los pacientes y en la inducción de efectos secundarios nocivos. Por estos motivos, el desarrollo de nuevas terapias más específicas y eficaces sigue siendo aún un objetivo científico prioritario a nivel mundial.

En este sentido, la inmunoterapia ha surgido como una alternativa prometedora en la lucha contra el cáncer. Desde el nacimiento de esta disciplina, en el siglo XIX, el interés en este campo se ha acrecentado exponencialmente a partir del año 2010. Los prometedores resultados obtenidos en ensayos clínicos han empujado a las agencias reguladoras de los medicamentos a la aprobación de diversos tratamientos basados en la inmunoterapia en los últimos años para su aplicación en clínica.

Concretamente, la inmunoterapia se basa en el refuerzo de la respuesta natural del sistema inmune que es responsable de la búsqueda, detección y eliminación de las células cancerosas. En los primeros estadíos de la enfermedad, el propio organismo posee la capacidad de frenar el desarrollo del tumor, pero éste adquiere en etapas más avanzadas la capacidad de pasar desapercibido para el sistema inmune. Es por ello que, aunque de forma natural no es capaz de evitar la implantación y el desarrollo de un cáncer, el sistema inmune se convierte en una diana terapéutica clave.

De manera particular, las células dendríticas se consideran la población celular más importante del sistema inmune, debido a que son las células presentadoras de antígeno más potentes, y a que enlazan de manera estratégica las dos principales ramas del sistema inmune: innata y adaptativa. Por una parte, son capaces de reconocer, capturar, procesar y presentar antígenos y de producir

citoquinas pro-inflamatorias en presencia de señales de peligro (o patrones moleculares asociados a patógenos, PAMPs por sus siglas en inglés). Por otra parte, tienen la habilidad de activar linfocitos T inmaduros tras la cross-presentación del antígeno, generando de esta manera potentes respuestas inmunitarias específicas de antígeno.

Las estrategias de inmunoterapia basadas en células dendríticas exploradas hasta la fecha pueden clasificarse en dos grandes categorías: las llevadas a cabo *in vivo* y *ex vivo*. Las estrategias *ex vivo* se basan en el aislamiento de células dendríticas del paciente, seguido de una manipulación en el laboratorio consistente en la expansión de células dendríticas, la carga con antígenos y la inducción de su maduración. Finalmente, las células son re-inyectadas en el paciente una vez su potencial de acción ha sido reforzado. Por el contrario, a lo largo de este trabajo se ha tratado de desarrollar una estrategia de inmunoterapia orientada a inducir la activación y maduración de células dendríticas *in vivo*. Para ello, se ha desarrollado una vacuna basada en agentes inmunoestimuladores cuya diana es la población de células dendríticas. Una vez activada esta población celular, se espera un efecto amplificado que incluya respuestas celulares de tipo citotóxico, que finalmente eviten el crecimiento del tumor, y de tipo memoria para proporcionar una inmunidad duradera frente al cáncer.

Dichos agentes inmunoestimuladores son agonistas de los receptores de tipo Toll (TLRs). Estos receptores se localizan en la membrana plasmática y en los endosomas de las células dendríticas (entre otras células del sistema inmune) y su función es la de reconocer PAMPs, entre los que se encuentran estructuras altamente conservadas a lo largo de la evolución como por ejemplo lípidos microbianos, carbohidratos, ácidos nucleicos o intermediarios de la replicación vírica. De esta manera, las células del sistema inmune pueden cumplir su función de centinelas frente a eventuales infecciones. Los agonistas de TLR elegidos son Poly(I:C) e imiquimod, dos moléculas sintéticas que activan, respectivamente, a los receptores TLR3 y TLR7. Se conoce que la combinación de diferentes ligandos de TLR provoca la activación y maduración de células dendríticas de manera sinérgica. Esto se traduce en la sobre-expresión de moléculas co-estimuladoras como CD80 y CD86, la secreción de citoquinas pro-inflamatorias y quimioquinas que atraen células T naïve y memoria y el aumento de los niveles del receptor de quimioquinas C-C de tipo 7 (CCR7), que promueve la migración de células dendríticas desde los tejidos periféricos hasta los órganos linfáticos, donde residen la mayoría de las células inmunes,

facilitando así la amplificación de la respuesta inmune. De esta manera, se puede considerar a la combinación de agonistas de TLR como potentes adyuvantes que podrían potencialmente incorporarse como componentes de una vacuna junto con el antígeno tumoral modelo ovalbúmina. La activación de linfocitos T requiere de tres señales: la interacción del complejo MHC-antígeno con el TRC; la co-estimulación por parte de proteínas de superficie de las células presentadoras de antígeno, que proporcionarían una señal reguladora (activadora o inhibidora) de la activación de células T; y la secreción de citoquinas que determinan la polarización de las células T inmaduras hacia los diversos fenotipos de linfocitos T maduros que existen ($CD4^+$, $CD8^+$, T_{reg} o Th17). La generación de potentes respuestas celulares $CD8^+$ específicas de antígeno son esenciales para la eliminación de las células tumorales, ya que esta población celular ejerce una acción citotóxica directa sobre células que son reconocidas como extrañas por el sistema inmune. De hecho, este tipo de respuestas son responsables de suprimir o retrasar el crecimiento de tumores *in vivo* en modelos animales experimentales vacunados siguiendo un esquema profiláctico y/o terapéutico.

A pesar de los beneficios que podría potencialmente aportar la inmunoterapia, su éxito también se encuentra limitado por diversas razones. Fundamentalmente, la administración de agentes inmunoestimuladores debe ser dirigida hacia los órganos y la población celular diana, en este caso los órganos linfáticos y las células dendríticas, respectivamente, para evitar desencadenar una respuesta inflamatoria inespecífica a nivel sistémico. Por otra parte, tanto el antígeno como el adyuvante deberían alcanzar a las células diana simultáneamente para inducir su correcta activación. Además, la administración sistémica de los componentes de la vacuna puede diluir la eficacia del tratamiento con dos consecuencias: primero, se requerirían repetidas dosis para conseguir una concentración farmacológicamente activa, y por otra parte, la acumulación en el organismo de compuestos con actividad farmacológica en altas concentraciones podría conllevar efectos tóxicos.

La nanotecnología ha surgido como un campo que ofrece aproximaciones prometedoras para complementar y potencialmente solventar las limitaciones a las que se enfrenta la inmunoterapia. El diseño de nanoparticulas permite controlar las propiedades que van a determinar su comportamiento dentro del organismo y por tanto, su aplicabilidad para el reconocimiento y eliminación de células cancerosas. Determinadas características de las nanoparticulas como el

tamaño, la carga, la forma, el material y las propiedades de superficie determinan su biodistribución, biocompatibilidad e inmunogenicidad, la capacidad de transportar y liberar compuestos terapéuticos de manera dirigida y controlada y la posibilidad de ser analizadas *in vivo* mediante técnicas de imagen molecular.

En esta tesis se ha propuesto como estrategia inmunoterapéutica el diseño de una vacuna basada en nanoparticulas de óxido de hierro y biofuncionalizadas con una combinación sinérgica de agonistas de TLR y un antígeno tumoral modelo con el objetivo de ser dirigidas de manera específica hacia el sistema inmune y generar así una eficaz respuesta inmune antitumoral.

Se conoce que el tamaño controlado de las nanoparticulas puede utilizarse como una estrategia de direccionamiento pasivo hacia los nódulos linfáticos. De esta manera, se potencia la inmunogenicidad del sistema mediante la liberación de compuestos immunoterapéuticos de forma dirigida a los órganos diana, evitando al mismo tiempo una posible toxicidad sistémica. Además, el empleo de sistemas agregados de un mayor tamaño también presenta una actividad inmunoestimuladora debido a la liberación sostenida de antígeno y adyuvante. La combinación de ambas estrategias podría, además, tener un efecto sinérgico.

La propia composición de las nanoparticulas asegura una elevada biocompatibilidad. Especialmente tres de los componentes empleados en la formulación: el hierro, un metal que interviene de manera natural en diferentes procesos fisiológicos; el polietilenglicol, un lípido ampliamente empleado en la industria farmacéutica debido a su alta biocompatibilidad y biodegradabilidad y a su baja toxicidad; y el imiquimod, un agonista de TLR7 actualmente aprobado por las agencias reguladoras de los medicamentos para su empleo en clínica para el tratamiento de varios procesos neoplásicos.

En cuanto a la interacción entre las nanovacunas y el sistema inmune, las nanoparticulas actúan como una plataforma para el co-transporte y liberación de antígeno y adyuvantes a una célula dendrítica diana y a un mismo compartimento celular, los endosomas, donde además se localizan los receptores TLR3 y TLR7. A su vez, durante el transporte los ligandos de TLR están protegidos por la nanoparticula frente a la degradación que pueden sufrir en su forma libre. Además, el transporte de antígeno y adyuvantes acoplados a una nanoparticula aumenta las probabilidades de que dichas biomoléculas sean endocitadas por las células presentadoras de

antígeno. La propia composición de la nanoparticula podría también actuar como un adjuvante *per se*. Concretamente, las nanoparticulas de óxido de hierro podrían desencadenar la polarización pro-inflamatoria del microambiente tumoral. El empleo de nanopartículas cargadas de compuestos bioactivos permite además la acumulación de dichas moléculas en una concentración biológicamente significativa de forma localizada, lo cual implica que las dosis requeridas para ejercer su acción son más bajas en comparación con la correspondiente forma libre, contribuyendo así a reducir la toxicidad asociada al tratamiento. En conjunto, estas características potencian el efecto del tratamiento con nanovacunas.

En esta tesis se han evaluado dos tipos de nanoparticulas de óxido de hierro: con y sin la superficie dopada con zinc. El dopaje mejora las propiedades de las nanoparticulas como agentes de contraste. Esta cualidad hace de este tipo de nanoparticulas un potencial candidato para la combinación de un agente diagnóstico y terapéutico en una misma plataforma. No obstante, en el diseño que proponemos en este trabajo la diana principal es el sistema inmune más que el propio tumor. En cualquier caso, permite su seguimiento *in vivo* y por consiguiente el análisis de su biodistribución mediante imagen por resonancia magnética. Concluimos que la biofuncionalización de las nanoparticulas modifica su distribución *in vivo*, sin afectar negativamente las propiedades inmunoestimuladoras del sistema.

El empleo de la combinación de ligandos de TLR Poly(I:C) e imiquimod como adyuvantes ha resultado ser extremadamente efectiva, hasta el punto de evitar el crecimiento de un modelo tumoral de melanoma durante varios meses tras la vacunación y subsiguiente inoculación del tumor. Además, la respuesta de memoria inmune generada es tan fuerte como para impedir el crecimiento del tumor tras una segunda inoculación. A pesar de la potencia de los adyuvantes, la nanoparticula contribuye acelerando y/o potenciando la generación de respuestas inmunes específicas de antígeno tanto de tipo celular como humoral.

Especial mención merece la actividad de la nanovacuna como agente terapéutico. En comparación con el enfoque profiláctico, la eficacia es razonablemente más limitada puesto que el sistema inmune carece del tiempo necesario para desarrollar la habilidad de responder de manera adecuada a una señal de peligro. No obstante, en términos relativos, es capaz de inducir un retraso en el crecimiento tumoral comparable con el que se consigue mediante ciertos

tratamientos quimioterapéuticos. En cualquiera de los casos, queda demostrada la capacidad de la vacuna para retrasar o impedir el desarrollo tumoral, así como de prolongar la supervivencia.

En definitiva, este trabajo pone en relieve la efectividad de una nueva vacuna basada en nanoparticulas como estrategia inmunoterapéutica aplicada al tratamiento del melanoma. Aporta como novedad el empleo simultáneo en la formulación de vacunas, por una parte, de nanoparticulas inorgánicas, y por otra parte, de una combinación sinérgica de ligandos de TLR, ambas estrategias aún poco exploradas. Por último, se sientan las bases para continuar explorando extensivamente nuevos y potentes adyuvantes aplicables a diferentes tipos de vacunas, así como la incorporación de nanomateriales para potenciar su efecto.

Summary

Tackling the treatment of such a complex disease as cancer represents, in many senses, a big challenge. In spite of the huge investment both in effort and money in cancer research during the last decades, this disease still remains being one of the main mortality causes in the developed countries. What is more, foresights point out that the incidence of this illness will continue rising in the future. In the particular case of melanoma, there is a tendency for increasing prevalence rates among the youngest population (< 30 years).

Traditional therapies are mainly based on the surgical resection of tumors, chemotherapy and radiotherapy. Nevertheless, the main limitations of these treatments are the lack of universality in the patient's response and the induction of harmful side effects. These are the reasons why the development of more specific and effective new therapies is nowadays a priority scientific goal worldwide.

In this sense, immunotherapy has emerged as a promising alternative in the fight against cancer. Since the beginning of this field, in the 19th century, it has been gaining interest exponentially since 2010. The promising results obtained in clinical trials have encouraged the drug regulatory agencies to license different immunotherapy-based treatments in the last years for their clinical application.

Immunotherapy aims the reinforcement of the natural response of the immune system responsible of seeking, detecting and eliminating cancer cells. During the first stages of the disease, the organism itself owns the ability to arrest tumors development, although they acquire in more advanced stages the capacity to avoid the immune recognition. For this reason, the immune system represents a key therapeutic target although it is frequently unable to avoid the implantation and development of a tumor by their means.

Dendritic cells are considered to be the most important cellular population of the immune system since they are the most potent antigen presenting cells and strategically connect the two main immunological branches: innate and adaptive. On the one hand, they are able to recognize, capture, process and cross-present antigens and release pro-inflammatory cytokines in the presence of danger signals (pathogen associated molecular patterns, PAMPs). On the other hand, they are able to activate naïve T lymphocytes after the cross-presentation of the antigen, thus generating potent antigen-specific immune responses.

The dendritic cell-based immunotherapeutic strategies developed until the date can be classified into two classes: *in vivo* and *ex vivo*. *Ex vivo* approaches are based on the isolation of the patient's dendritic cells followed by their expansion, antigen loading and maturation *in vitro*. Finally, cells are reinfused to the patient once their potential activity has been reinforced. By contrast, along this work we have attempted to develop an immunotherapeutic strategy guided to promote the activation and maturation of dendritic cells *in vivo*. With this purpose, we have developed a vaccine based on immunostimulatory agents whose target is the dendritic cell population. Once activated, we aim to elicit an amplified effect including cytotoxic cellular responses that ultimately avoid the tumor growth, as well as memory responses to provide a durable immunity against cancer.

Such immunostimulatory agents are Toll-like receptors (TLRs) agonists. These receptors are located on the plasmatic membrane and endosomes of dendritic cells (among other immune cellular populations) and their role is the recognition of PAMPs. Some examples of PAMPs are certain structures highly evolutionarily conserved such as microbial lipids, carbohydrates, nucleic acids and mediators of viral replication. This way, the cells of the immune system act as sentinels against eventual infections. The selected TLR agonists are Poly(I:C) and imiquimod, two synthetic molecules that engage TLR3 and TLR7, respectively. It has been reported that the combination of different TLR agonists triggers the activation and maturation of dendritic cells in a synergistic manner. It involves the overexpression of co-stimulatory molecules such as CD80 and CD86, the release of pro-inflammatory cytokines and chemokynes that attract naïve and memory T cells and the upregulation of the C-C chemokine receptor 7 (CCR7) that promotes the migration of dendritic cells from the peripheral tissues to the lymphatic organs, where most immune cells reside, thus enabling the amplification of the immune response.

The combination of TLR agonists may be considered as a potent adjuvant which could potentially be incorporated as a vaccine component along with the tumoral model antigen ovalbumin. The activation of T lymphocytes requires three stimuli: the interaction between the complex MHC-antigen and the TCR; the co-stimulation by surface proteins of the antigen presenting cells, which provide a regulatory signal (positive or negative) for the activation of T cells; and the release of cytokines that determine the differentiation of immature T cells towards the diverse T lymphocyte phenotypes ($CD4^+$, $CD8^+$, T_{reg} or Th17). The generation of potent

antigen-specific $CD8^+$ cellular responses is essential for the eradication of tumors, since this cellular population exerts a direct cytotoxic activity on cells recognized by the immune system as strange ones. In fact, this kind of responses is responsible of the suppressed or delayed tumors growth *in vivo* in experimental animal models immunized following a prophylactic and/or therapeutic schedule.

In spite of the potential benefits of immunotherapy, its success is limited due to different reasons. Importantly, the administration of immunostimulatory agents has to be guided to the target organs and cellular population (in this case the lymphatic organs and dendritic cells, respectively) in order to avoid a systemic unspecific inflammatory response. Furthermore, both the antigen and the adjuvant should reach the target cell simultaneously to induce a proper activation. Moreover, the systemic administration of the vaccine components may diminish the efficacy of the treatment with two consequences: first, repeated doses would be required to reach a pharmacologically active concentration and, on the other hand, the accumulation of high concentrations of compounds with pharmacologic activity inside the organism could result in toxic effects.

Nanotechnology has emerged as a field that offers promising approaches to complement and potentially solve the limitations of immunotherapy. Nanoparticles engineering allows the fine tuning of the properties that determine their behavior inside the organism and so, their applicability for the recognition and elimination of tumor cells. Certain features of the nanoparticles, such as size, charge, shape, composition and surface properties determine their biodistribution, biocompatibility and immunogenicity, their ability to transport and deliver therapeutic compounds in a targeted and controlled manner as well as the possibility to be tracked *in vivo* through molecular imaging techniques.

In this thesis, we propose as an immunotherapeutic strategy the design of a vaccine based on iron oxide nanoparticles biofunctionalized with a synergistic combination of TLR agonists and a model tumoral antigen to specifically target the immune system, thus generating an effective antitumoral immune response.

It is known that the controlled size of nanoparticles can be used as a passive targeting strategy towards the lymph nodes. This way, the immunogenicity of the system is potentiated through the

release of immunotherapeutic drugs directly to the target organs, avoiding at the same time a possible systemic toxicity. Moreover, the employment of aggregated systems with a higher diameter also shows an immunostimulatory activity due to the sustained release of antigen and adjuvant. In addition, the combination of both strategies could have a synergistic effect.

The nanoparticle composition ensures a high biocompatibility. Particularly, three of the compounds employed in the vaccine formulation: iron, a metal naturally involved in different physiologic processes; polyethylene glycol, a lipid commonly used in the pharmaceutical industry due to its high biocompatibility and biodegradability and its low toxicity; and imiquimod, a TLR7 agonist currently approved by the regulatory drugs agencies for its clinical application in the treatment of several neoplasic diseases.

Regarding the interaction between the nanovaccines and the immune system, nanoparticles act as a platform for the simultaneous transport and co-delivery of antigen and adjuvant to a unique targeted dendritic cell and to the same intracellular compartment, the endosomes, where TLR3 and TLR7 are located. Furthermore, TLR ligands are protected by the nanoparticle against the degradation they may undergo in their soluble forms during the transportation. Moreover, the attachment of antigen and adjuvants to a nanoparticle increases the probability for those biomolecules to be endocytosed by antigen presenting cells. The nanoparticle composition might act as an adjuvant *per se*. In particular, iron oxide nanoparticles can induce the pro-inflammatory polarization of the tumor microenvironment. The employment of nanoparticles loaded with bioactive compounds also enables the accumulation of such molecules in a biologically significant concentration in a localized manner, meaning that the doses required to exert their action are lower than those required by the soluble counterparts, thus contributing to reduce the toxicity associated to the treatment. Altogether, these characteristics boost the effect of the nanoparticle-based treatments.

In this thesis we have evaluated two kinds of iron oxide nanoparticles: with and without a zinc-doped surface. The doping improves the properties of the nanoparticles as contrast agents. This feature makes them a potential candidate for the combination of a diagnostic and a therapeutic agent on the same platform. Nevertheless, the main target we propose is the immune system rather than the tumor. In any case, it is a characteristic that enables their tracking *in vivo* and, consequently, the analysis of their biodistribution through magnetic resonance imaging. We

conclude that the biofunctionalization modifies nanoparticles *in vivo* distribution, without adversely affecting the immunostimulatory properties of the system.

The combination of TLR agonists Poly(I:C) and imiquimod as vaccine adjuvants has turned to be extremely effective, to the point of avoiding the development of a melanoma tumor model for several months after the immunization and subsequent tumor inoculation. Moreover, the memory immune response generated is strong enough as to inhibit tumor growth after a second challenge. Despite the potency of the adjuvants, the nanoparticle contributes accelerating and/or potentiating the onset of both cellular and humoral antigen-specific immune responses.

The activity of the nanovaccine as a therapeutic agent deserves a special mention. Compared to the prophylactic approach, the efficacy is reasonably more limited as the immune system lacks the time necessary for developing the ability to respond appropriately against a danger signal. Nevertheless, in relative terms, it is able to induce a delayed tumor growth similar to the one achieved through certain chemotherapeutic treatments. In any case, the ability of the vaccine to the delay or avoid the tumor development and to extend mice survival has been demonstrated.

Definitely, this work highlights the effectiveness of a new nanoparticle-based vaccine as an immunotherapeutic strategy applied to the treatment of melanoma. As a novelty, it combines on the same vaccine formulation inorganic nanoparticles, on the one hand, and a synergistic combination of TLR agonists on the other hand, both strategies scarcely explored until the date. Finally, it opens an avenue for a deeper assessment of new and potent adjuvants applicable to different kinds of vaccines, as well as the incorporation of nanomaterials to boost their effect.

Chapter 1

General introduction

This initial chapter aims to contextualize and provide the general background of this PhD thesis and the research project carried out. It provides a brief overview of the fields of cancer immunotherapy and cancer nanomedicine, and describes and discusses the state-of-the-art, challenges and opportunities in the development of nanoparticle-based anti-cancer vaccines.

1.1. Immunotherapy.

1.1.1. Definition and history.

The term immunotherapy refers to the reinforcement of the host immune system in order to trigger an endogenous anti-tumor response. In the earliest stages of the neoplastic process, mutated proteins, known as 'neoantigens', are generated and presented on the surface of tumor cells. These antigens are recognized by professional antigen presenting cells (APCs) and cross-presented to T lymphocytes. The interaction between the TCR of T-cells and the complex MHC-antigen of APCs, together with additional co-activation signals, ultimately leads to the activation of an anti-tumor immune response. In this way, the host immune system can avoid the development of cancer during the early stages. Nevertheless, the tumor develops distinct resistance mechanisms in order to escape from the immune surveillance and destruction. The most relevant mechanisms are the establishment of a strong immunosuppressive tumor microenvironment, the inhibition of T-cells activity and the progressive generation of poorly immunogenic and/or apoptosis-resistant tumor cells. These tumor-escape mechanisms have compromised the efficacy of immunotherapeutic strategies.

The birth of immunotherapy dates back to the 19th century, when William B. Coley successfully triggered an anti-tumor immune response against sarcoma after the local administration of bacteria-derived toxins into the patients. Since then, several attempts have aimed to stimulate immune-related responses to fight against cancer. For instance, the injection of cytokines such as IL-2 or IFNα has been applied in cancer treatment for several decades. However, recent advances since 2010 are giving back immunotherapy the deserved relevance [1]: the approval by the FDA of the first autologous cellular immunotherapy, sipuleucel-T, for the treatment of prostate cancer in 2010; the approval of anti-CTLA-4 (ipilimumab) and anti-PD-1 (nivolumab) antibodies in 2011 and 2014 respectively; and the combination of both antibodies for the treatment of melanoma in 2015.

1.1.2. Immunotherapeutic strategies.

Before defining the place of this thesis in the vast immunotherapy field, a general overview of the different cancer immunotherapy approaches will be given [2–4]:

- Strategies to activate effector T-cell responses.

    - *Vaccination with neoantigens.*

      It consists on the administration of tumor associated antigens (TAAs), either in the form of full-length recombinant proteins, synthetic peptides, whole tumor cells or tumor cell lysates. The most important and challenging issue is the isolation of the most appropriate antigen or, alternatively, the supply of an antigen source which provide the most varied epitope profile possible. GVAX, the most promising approach currently under development, is a vaccine consistent on an entire tumor cell as a source of antigens, genetically modified to release the cytokine GM-CSF and irradiated to avoid further proliferation [5].

    - *Vaccination with antigen plus adjuvant.*

      The main limitation of a vaccine composed solely by antigens is the inadequate activation of dendritic cells (DCs). This cellular population plays a key role in the coordination of innate and adaptive immune responses. Therefore, their activation and maturation is essential in order to trigger potent responses that overcome the ability of the tumor to induce immune tolerance. To do so, several strategies have been designed based on the activation of innate immune signaling pathways involved in the activation of DCs through the release of interferons (IFN) and other pro-inflammatory cytokines as well as through the overexpression of several co-stimulatory signals. As an example, the employment of Toll-Like Receptors (TLR) and Stimulator of Interferon Genes (STING) agonists is an available strategy to trigger innate mechanisms of defense against pathogens since those molecules show a potent adjuvanticity that reinforces the effect of the vaccines [6, 7].

- *Virotherapy.*

  It is based on the use of natural or genetically engineered viruses that selectively infect and ultimately cause lysis of tumor cells with minimal disturbance of normal cells. Apart from the direct oncolytic activity, the virus-induced cell death releases virus progeny, Pathogen Associated Molecular Patterns (PAMPs), Damage Associated Molecular Patterns (DAMPs) and Tumor-Associated Antigens (TAAs) that trigger a systemic anti-tumor response. To date, only one virotherapy drug has been approved by the FDA and the EMA for the treatment of advanced melanoma, Talimogene laherparepvec (T-VEC) [8, 9].

- Strategies to neutralize immunosuppressor mechanisms.

  - *Immune checkpoint blockade.*

    Immune checkpoints are inhibitory receptors whose activation impedes T-cell function [10]. Their physiological role is to balance the magnitude of immune responses to avoid damage to the own tissues, as well as to avoid reactivity to self-antigens. However, tumors employ immune checkpoints as a mechanism of immune evasion. Then checkpoint blockade, understood as the blockade of immune inhibitory pathways activated by tumor cells, is being used as a successful therapeutic strategy. To date, five monoclonal antibodies have been approved by the FDA for their clinical use: anti-CTLA-4 (Ipilimumab), anti-PD-1 (Nivolumab and Pembrolizumab) and anti-PD-L1 (Atezolizumab and Durvalumab) antibodies [11, 12].

  - *Alternative checkpoint inhibitors.*

    Several alternative immune checkpoints are currently under investigation for potential use in advanced cancer. Two of them, Lymphocyte Activation Gene 3 (LAG3) and T cell Immunoglobulin 3 (TIM3), are proteins expressed on the surface of exhausted T cells. Their inhibition might overcome T cell anergy, leading to oncolytic responses. Killer immunoglobulin-like receptors (KIRs) are

immune checkpoints of NK cells that have also gained attention because their blockade prevents the recognition of HLA molecules, thus triggering the destruction of tumor cells by NKs in an antigen-independent manner [13].

- *Inhibition of immunosuppressive tumor microenvironment.*

  The enzyme indoleamine 2, 3-dioxygenase (IDO) is involved in the maintenance of the immunosuppressive tumor microenviroment through T_{reg} activation and $CD8^+$ T cells inhibition. Therefore, the targeted blockade of IDO is an interesting therapeutic approach currently under development.

- Supply of agonists of co-stimulatory signals.

The alternative to the blockade of inhibitory signaling pathways in T cells is the activation of co-stimulatory receptors, such as CD137, OX40, CD40 or GITR. In this case, monoclonal antibodies have been designed and applied as selective agonists of such receptors, thus triggering anti-tumor cellular responses.

- Cell-based therapies.

  - *Tumor-infiltrating lymphocytes (TILS).*

    CTLs and Th cells are isolated from the tumor and cultured *ex vivo* in order to expand tumor antigen-specific cellular populations that are physiologically repressed in the tumor microenvironment. After a chemotherapy or radiotherapy-based lymphodepletion that aim the destruction of immunosuppressive cellular populations in the tumor such as T_{reg} or MDSCs, activated TILs are reinfused back to the patient, resulting in the tumor rejection [14].

  - *DC-based vaccines.*

    This therapy is based on the extraction of DCs from the patient's peripheral blood, followed by their activation and antigen loading *ex vivo* and the subsequent

readministration to the patient. The first adoptive cell therapy approved, Sipuleucel-T, is based on DCs and is applied to prostate cancer treatment. In this case, this cellular population is genetically modified to express a prostate cancer antigen and a recombinant protein which encodes a prostatic acid phosphatase and the cytokine GM-CSF [15].

- *TCR transfer.*

  This approach involves the genetic engineering of T-cells to express the α and β chains of the T cell receptor (TCR), which confers them the ability to specifically recognize neoantigens presented by tumors through the HLA/MHC complex [16].

- *Chimeric antigen receptor therapy (CART).*

  It is a variation of the latter strategy that overcomes its main limitation: the down-regulated expression of HLA by tumor cells as an immune evasion mechanism. Chimeric antigen receptors are constituted by an Ig variable domain fused to a TCR constant domain. The fragment of the protein derived from the variable chains of an antibody ensures the recognition of neoantigens with a high specificity in a HLA-independent manner [17–19]. Kymriah® (tisagenlecleucel), the first CART-based therapy approved by the FDA, was recently licensed (in August of 2017) for the treatment of a pediatric form of acute lymphoblastic leukemia [20]. It is a genetically-modified autologous T cell immunotherapy, by which the patient's T cells are isolated and genetically modified to insert a new gene that codifies a specific protein (a chimeric antigen receptor or CAR) that directs T cells against leukemia cells that show a particular antigen (CD19) on the surface. Once modified, T-cells are reinfused back to the patient.

1.1.3. Vaccines: state-of-the-art, current limitations and future prospects.

Our position in the promising and challenging immunotherapy field is the anti-cancer vaccine approach. The strategy proposed in this thesis is based on the co-delivery of an antigen and a synergistic combination of TLR agonists as adjuvants using inorganic nanoparticles as delivery

platforms applied to the treatment of a melanoma tumoral model.

In general, there are two types of anti-cancer vaccines: prophylactic (or preventive) and therapeutic (or healing) vaccines, depending on whether their administration is prescribed before or after the appearance of the malignancies, respectively. Prophylactic vaccines aim to develop immunological memory in healthy subjects to prevent the appearance of a disease. Certain chronic viral infections, such as human papillomavirus (HPV), hepatitis B and C viruses (HBV and HCV), Epstein-Barr virus (EBV) and *Helicobacter pilori*, are related to carcinogenesis. To date, only three prophylactic vaccines against virus-related carcinomas have been approved by the FDA: Gardasil® and Cervarix® for the prevention of cervical cancer (HPV) and Fendrix® against liver cancers resulting from the sustained infection of the hepatitis B virus [21].

Conversely, therapeutic vaccines aim to raise an immune response against an ongoing disease. In the case of cancer, the goal is to arrest tumor growth and prevent subsequent relapses. Apart from the FDA-approved Sipuleucel-T, Kymriah, T-VEC, anti-CTLA-4 and anti-PD-1 monoclonal antibodies previously mentioned, several immunotherapeutic strategies are currently undergoing pre-clinical or clinical trials [22]. Several examples of anti-cancer vaccines in the same line of our research can be found on databases about clinical trials. For instance, a variety of HER-2 derived synthetic peptides were administered in combination with Hiltonol, a variant of the TLR3 agonist Poly(I:C) with improved stability, to breast cancer patients in a clinical trial that was terminated with irrelevant immune responses to the vaccine [23]. Applied to lung cancer, Tecemotide, which is a liposomal vaccine composed by a synthetic MUC-1 derived peptide adjuvanted with the TLR4 agonist MPLA [24], demonstrated in a phase III clinical trial a clinical benefit in terms of improved survival to patients that received simultaneously chemotherapy and radiotherapy prior to the immunization [25]. The two TLR agonists used in this thesis, Poly(I:C) (TLR3) and imiquimod (TLR7), are currently being used separately in different clinical trials, but the combination of both TLR agonists, as well as any other TLR combination, still remains unexplored outside pre-clinical context. The use of imiquimod by itself for the treatment of viral external genital lesions (HPV papillomas), genital and perianal warts, superficial basal cell carcinoma and actinic keratoses was approved by the FDA in 2004 and is clinically used nowadays [26]. Iron oxide nanoparticles (ferumoxytol, Feraheme®) are in turn being used and investigated in the context of magnetic resonance imaging (MRI), but not as components of

immunotherapeutic vaccines. Several authors have reported the successful application of nanoparticles loaded with a combination of TLR agonists for the induction of effective antigen-specific cellular responses, improved pro-inflammatory cytokine release profiles and stronger antibody-mediated responses [27–30]. The same approach was analyzed in the context of anti-cancer vaccines by Kornbluth *et al* [31] and Florindo *et al* [32], who demonstrated a significant B16F10 tumor growth delay and improved survival in immunized mice. However, the development of magnetic nanoparticle-based multicarriers of TLR agonists as anti-cancer vaccine adjuvants still remains completely unexplored.

Anti-cancer vaccines face several obstacles that hinder the development of successful treatments. An important issue is the immune-related toxicity. The therapeutic exacerbation of T-cell responses as well as the disruption of mechanisms that balance the magnitude of immune responses leads to the proliferation of immune cellular populations whose physiological role is the immune suppression, such as T_{reg} and MDSCs. This could eventually lead to an accelerated tumor growth or to the transient inhibition of endogenous anti-tumor responses [33]. Nevertheless, the undesirable side effects inherent to any treatment only limit its applicability when the degree of severity of the clinical symptoms is considered unacceptable.

However, one of the main and most challenging obstacles is in the identification of the most appropriate antigen(s) to drive immune responses specifically against the tumor. In general, tumor cells show a poor antigenicity due to the down-modulated expression of MHC complexes, which is one of the mechanisms of tumor escape from immune surveillance. Apart from that, they show a heterogeneous antigen expression as a result of the antigenic variations generated by the process called 'cancer immunoediting', which avoids the implementation of universal strategies. Finally, most tumor antigens are self-proteins, therefore they would be accepted (tolerated) by the host immune system as self-antigens. Three problems that point out to the crucial importance of identifying tumor-associated antigens (TAAs) that are recognized by the immune system as strange and aberrant proteins. Several TAAs have been identified resulting from mutations in oncogenes or oncosuppressor genes (e.g. BRCA1, BRCA2, HER2), developmental antigens (e.g. MAGE, melan-A, gp100), antigens upregulated during malignant transformation (e.g. CEA) and viral antigens associated with oncogenesis [21]. Different approaches have been assessed in order to tackle the problem of antigen choice. First, the

administration of whole tumor cells or tumor cell lysates provides a wide variety of tumoral antigens. Despite being an excellent antigenic source, this strategy still needs to solve problems related to safety and self-reactogenicity. Subunit vaccines have emerged as a promising alternative since synthetic peptides can be inexpensively produced at large scale, easily administered to patients and allow monitoring antigen-specific immune responses [21]. To face the problem of antigen heterogeneity, polyvalent vaccines provide several of the most frequent epitopes of the TAAs related to a particular type of cancer, thus increasing their effectiveness. They can be constituted by full length proteins or a pool of antigenic peptides. Monovalent vaccines that contain only one antigen with narrow epitope specificity correlate with low success rates in clinical trials [22]. Nevertheless, some authors report that the immunization with a unique antigen might lead to the onset of immune responses against other TAAs [34]. While the convenience of using a single antigen is not clear yet, the necessity of incorporating one or several adjuvants to the vaccine formulation is widely accepted, since synthetic purified antigens are poorly immunogenic.

Other parameters that limit the development of effective anti-cancer vaccines are related to the optimization of the schedule, dosing and route of administration of the vaccine, the choice of suitable adjuvants and delivery vehicles and the optimal strategy to induce the activation and maturation of DCs.

Current trends in research that define the future development of vaccines are related to different topics [22, 33]:

- The employment of delivery platforms that possess inherent immunogenic properties such as viral vectors, liposomes or pathogen-like micro- or nanoparticles.

- The discovery of new potent adjuvants that preferentially activate Th1 and CTL responses.

- Development of immunotherapeutic strategies in the context of multimodal treatments that combine tumor surgical resection, chemotherapy, radiotherapy and immunotherapy with potential synergistic mechanisms of action.

- Definition of predictive biomarkers that enables the selection of patients with a higher

probability of developing a successful response to a particular treatment. This would allow the clinicians to decide the most appropriate treatment strategy in a personalized manner.

1.2. Nanoparticles in nanomedicine and for the development of nanovaccines in cancer immunotherapy.

Magnetic nanoparticles are already used for a variety of applications in nanomedicine [35, 36]:

- Controlled magnetic transport and immobilization of cells and biological materials. The magnetic properties of iron oxide nanoparticles are useful for tagging biological materials of interest, as well as living cells, and subsequently immobilizing or moving them towards the region of interest using a magnetic field gradient [37]. This application has also an interest for the isolation of concentrated samples for further manipulation or analysis *ex vivo* [38–40].

- Targeted drug delivery. Related to the previous application, in this case the magnetic nanocarriers provide targeted delivery of chemotherapeutic drugs or diagnostic radioactive probes to a particular region within the body, such as a tumor, taking advantage of the penetrability of magnetic fields into mammals' tissues and avoiding undesirable off-targeted side effects [41, 42]. Magnetofection is the delivery of genetic material inside target cells for gene therapy based on the same principles.

- Hyperthermia treatments. Nanoparticles are directed to the cancerous tissue and exposed to a magnetic field with a strength and frequency enough as to generate heat. Tumor cells exposed to a high temperature (> 40 °C) for a long time (> 30 min) are destroyed [43, 44].

- Magnetic resonance imaging (MRI) contrast enhancement. Iron oxide nanoparticles provide excellent contrast agents for MRI for several reasons: high biocompatibility and differential uptake for different tissues (preferentially liver and reticuloendotelial system) in a size-dependent manner. They can also act as

multimodal imaging devices and as labels for *in vitro* and *in vivo* cellular tracking [45–48].

1.2.1. Advantages of particulate vaccines.

The use of cytokines and TLR agonists (TLRa) to induce the activation and maturation of DCs avoids the disadvantages of DC-based vaccines, which as an adoptive cell therapy requires the isolation and manipulation DCs *ex vivo,* and therefore presents safety issues, is time consuming and expensive. Nevertheless, apart from the aforementioned obstacles to the development of successful anti-cancer vaccines (immunosuppressive tumor microenvironment, potential toxicity, poor antigenicity), the clinical success of these vaccines is restricted partly due to the toxicity associated to the systemic release of TLR agonists and the reduced effectiveness of a non-targeted delivery to DCs. This hurdle can potentially be overcome by the use of particle-based delivery vehicles. The development of particulate vaccines provides a range of advantages:

- The controlled release of the vaccine components to the target cells allows the employment of low dosages that reduce potential toxic side-effects. The local concentration reached at the target organs is significantly higher for nanoparticulate drugs than with the same drugs in solution [49].

- Certain parameters enable the reduction of antigen and adjuvant quantities required to exert an immunological effect. Parameters that can be optimized to improve the efficacy and safety of the vaccine include the nanoparticle size and composition, the surface modification with ligands that target DCs and the addition of capping ligands that modify the biodistribution of nanoparticles or facilitate their drainage and/or retention into the lymphatic system [50].

- The high surface-area-to-volume ratio allows the attachment of a variety of ligands and drugs [51].

- The attachment of antigen and adjuvants to nanocarriers protects them from proteasomal degradation [29].

- The delivery of TLRa on nanoparticles improve their safety profile, allow the use of potent adjuvant combinations and enable the employment as adjuvants of small

molecules with poor pharmacokinetics [52].

- APCs efficiently internalize nanoparticles both through passive and active targeting. Consequently, even non-targeted nanoparticles enhance the uptake of the ligands they carry compared to their soluble forms.
- Nanoparticles allow the simultaneous intracellular presence of both antigen and adjuvant, boosting the efficacy of the treatment and mediating the polarization of the immune responses elicited.

As a strategy, targeting the immune system instead of directly attacking tumor cells is more effective for several reasons [51]. First, whereas guiding nanoparticles to the tumor after a systemic administration is rather challenging, it is possible to accumulate them in lymphoid organs, where most APCs are located, both through passive and active targeting [53, 54]. It has been estimated that only 0.7 - 0.9 % of the total nanoparticle dose injected ultimately reaches the tumor [55] in spite of the contribution of active tumor targeting strategies such as the coupling to nanoparticles of ligands such as aptamers, transferrin, folic acid, EGFR ligands or integrin-binding peptides and the employment of anti-HER2 and anti-VEGF monoclonal antibodies [56, 57]. Second, lymphoid organs (particularly the spleen) are more permeable structures than tumors due to the lack of the physical barriers characteristic of solid tumors, such as a high interstitial pressure or a high-density extracellular matrix [51]. Although nanoparticles may penetrate the tumors through passive diffusion and accumulate inside them as a result of the leaky vasculature in the tumor tissue and a poor lymphatic drainage (the so called enhanced permeability and retention (EPR) effect), the reticuloendothelial and renal systems compete with the tumor for circulating nanoparticles and sequester or eliminate up to 99% of them [58, 55]. Third, the magnitude of the immune responses is highly amplifiable. It means that while tumor cells require to be exposed to high doses of oncolytic drugs to be killed, even a low quantity of an immostimulating agent may trigger the onset of a strong anti-cancer immune response [50]. In terms of designing a therapeutic nanocarrier, it is quite relevant as the amount of ligands to be loaded on the nanoparticle is much higher in the case of chemotherapeutic agents. Fourth, the generation of a memory response to prevent subsequent relapses is only possible for immunotherapies. Finally, in the majority of

nanoparticle-based therapeutic approaches, the immune system is an obstacle since the phagocytes of the reticuloendothelial system rapidly remove nanoparticles from the systemic circulation, thus hindering their action [59].

1.2.2. Engineering nanoparticle-based vaccines: state-of-the-art, current limitations and future prospects.

Engineering of nanoparticle-based vaccines relies on the cooperation between materials science and immunology. The design of immunoactive biomaterials requires a deep understanding of the physicochemical properties of the materials and the general functioning of the immune system in order to elucidate issues such as the host-material interactions or the spatiotemporal distribution of nanoparticles, antigen and adjuvants, as well as the biological responses they elicit.

Nanoparticles have sizes in the range of different biological entities such as viruses (10-200 nm) or proteins (2-15 nm) [60]. Several kinds of nanoparticles are being used for the development of vaccines (**Table 1.1**). These nanoparticles can be engineered to resemble pathogen-mimetic structures such as immune protein complexes, viruses or bacteria (**Figure 1.1**).

Particle	Characteristics and Mechanisms	Size	Commercial Name
Emulsions	Oil in water emulsions composed of a solvent and a surfactant. Vaccine adjuvant, leads to recruitment of immune cells and induction of Th1 response.	50–600 nm	MF59™, Montanide™
Inorganic NPs	Rigid structure and controlable synthesis. Non-biodegradable.	0.8–200 nm	AuNPs (Gold), Fulleren
ISCOM	Immune-stimulating complex."Cage-like" particles. Popular ISCOMs are made of saponin, cholesterol and phospholipds.	40 nm	ISCOM, ISCOMATRIX
Lipid-based NPs	Biodegradable lipidic NPs such as liposomes, micelles and solid lipids nanoparticle. Encapsulation of antigens with controlled release.	200–1000	DOTAP
Polymeric NPs	Synthetic polymers. Allows controled release of antigens or drugs. Biodegradable.	Variable	PLG, PEG, polystyrene
Carbohydrates	Natural polysaccharide. Shape and size are easily manipulated with impact on the profile of the immune response. Biodegradable.	Variable	Pullulan, Advaxa™ (Inulin)
Self-assembled proteins	Self-assemblying proteins that fold into complex quartenary structure.	10–40 nm	Ferritin, MVP.
Viral Vectors	Efficient gene transfer for transiente of stable expression. Induce robust CTL responses. Good safety and tolerability profile from clinical trials in humans.	Variable	MVA, Adeno
VLPs	Self-assembled viral capsides devoided of infectious nucleic acid. Confers viral fingerprint to displayed antigens.	15–50 nm	Gardasil, Cervarix.

VLPs: Virus-Like Particles; CTL: Cytotoxic T Lymphocytes; NPs: Nanoparticles; ISCOMs: Immune-stimulating complex; Th1: T helper 1.

Table 1.1. *Classification of nanoparticles used in nanovaccines according to their composition. Taken from Bachmann et al* [61].

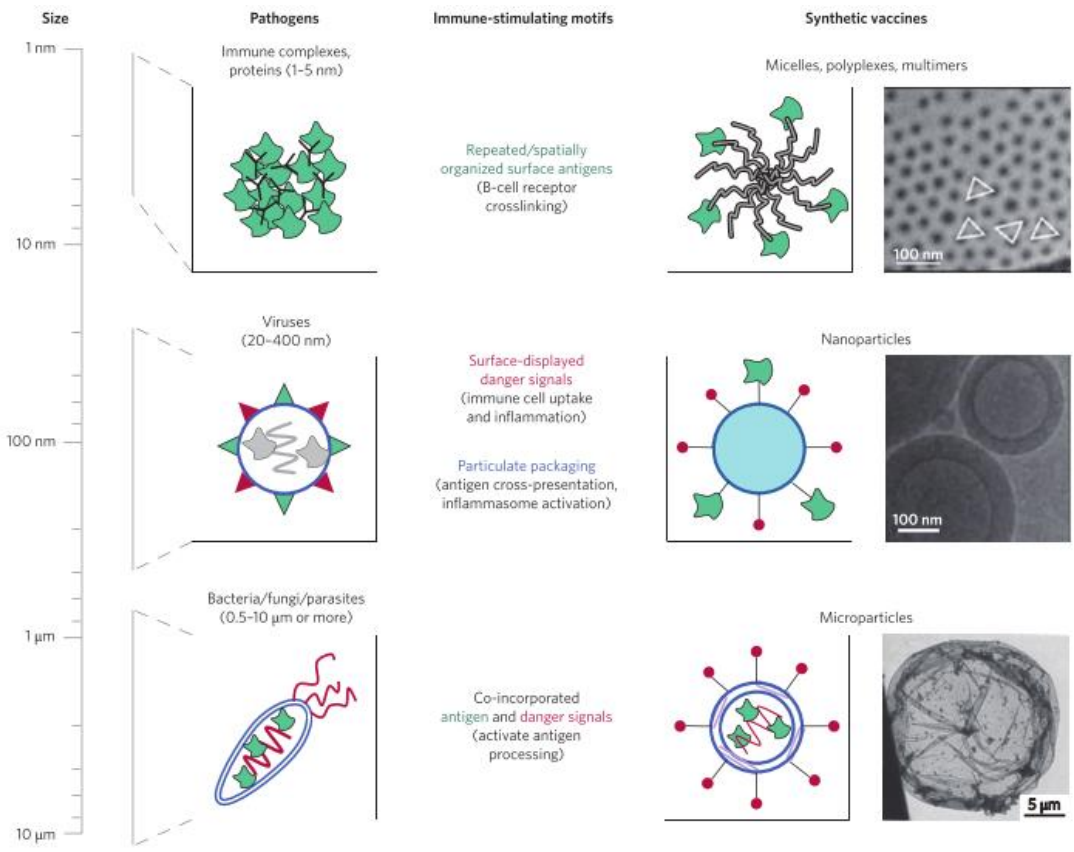

Figure 1.1. *Biomaterial-base vaccines engineered to resemble naturally occurring pathogens. Taken from Irvine et al* [52].

For example, antigenic molecules (usually peptides) and adjuvants such as PAMPs can be associated to nanomaterials in different ways [62, 63]. In general, the interaction of biomolecules with nanoparticles can be classified in the following way: chemical conjugation to the nanoparticle surface; encapsulation inside nanospheres; adsorption to the surface through non-covalent interactions; and simple mixtures of biomolecules and biomaterials. Adopting one of these strategies, or a combination of several of them, it is possible to develop pathogen mimicking structures. For instance, virus-like particles (VLPs) which are constituted by a self-assembled proteic nanoparticle (20-100 nm in size) resembling a virus capsid and selected antigenic proteins conjugated to the surface have been used for decades in vaccines such as those against hepatitis B (HBV) and human papillomavirus (HPV). Other approaches are currently under investigation. As an example, Fahmy *et al* proposed a biomimetic nanoparticle (around

300 nm in diameter) made of the biodegradable polymer PLGA and functionalized with MPLA, CpG and OVA resembling the bacterial cell wall, the pathogen genome and an intracellular antigenic protein, respectively [29]. Remarkably, the only kind of nanoparticle licensed as a human vaccine to date are VLP-based vaccines. Apart from Fendrix®, Gardasil® and Cervarix® (in use since the early 1980s, 2006 and 2007, respectively), a fourth VLP-based vaccine against hepatitis E was licensed in China in 2011 [61]. Based on the promising results obtained in advanced clinical trials, in 2015 the European Medicines Agency (EMA) adopted a positive scientific opinion about the anti-malaria vaccine candidate developed by GlaxoSmithKline under the trade name of Mosquirix® [64]. Pilot implementation of this vaccine is expected to start in the coming years. Apart from VLP-based vaccines, only two other nanomedicines are currently approved: Doxil, a liposomal formulation of doxorubicin, and Abraxane, an albumin-bound nanoparticle of paclitaxel [49]. Overall, it is reasonable to state that despite a number of successes the implementation of nanoparticle-based therapies is still in its early days.

The ways by which a pathogen-like nanoparticle interacts with the host immune system to trigger an antigen-specific immune response are diverse [60,61,65,66] and all can be useful for nanoparticle-based vaccine engineering (**Figure 1.2**). First, nanoparticles improve antigen uptake by professional antigen-presenting cells (APCs) compared to the soluble forms or microparticles. This strategy is likely to be the most effective one in terms of activation of effector cellular responses. The particle size also determines the migration of antigen-loaded nanoparticles from the periphery to the lymphatic system, enabling the co-delivery of antigen and adjuvants to relevant cellular populations. In general, nanoparticles of < 2 nm in diameter can penetrate blood vessels, whereas the optimal size to spontaneously reach the draining lymph nodes is around 10-50 nm [52]. Larger nanoparticles can also directly diffuse to lymphatic organs with a diminished rate or indirectly through peripheral circulating macrophages, which facilitate their transport to DCs [54].

Large particles or nanoemulsions are retained at the site of injection, acting as biomaterial scaffolds that attract APCs to a matrix containing immunogenic material rather than as delivery vehicles that transport that material to the target cells [60]. This phenomenon, known as 'depot effect', enables a sustained and prolonged antigen release. Furthermore, the pro-inflammatory activity of this approach is also related to the local release of cytokines and chemokines, the

recruitment of immune cellular populations and the up-regulated expression of CC-chemokine receptor 7 (CCR7) in DCs, which mediate their translocation to the draining lymphoid organs.

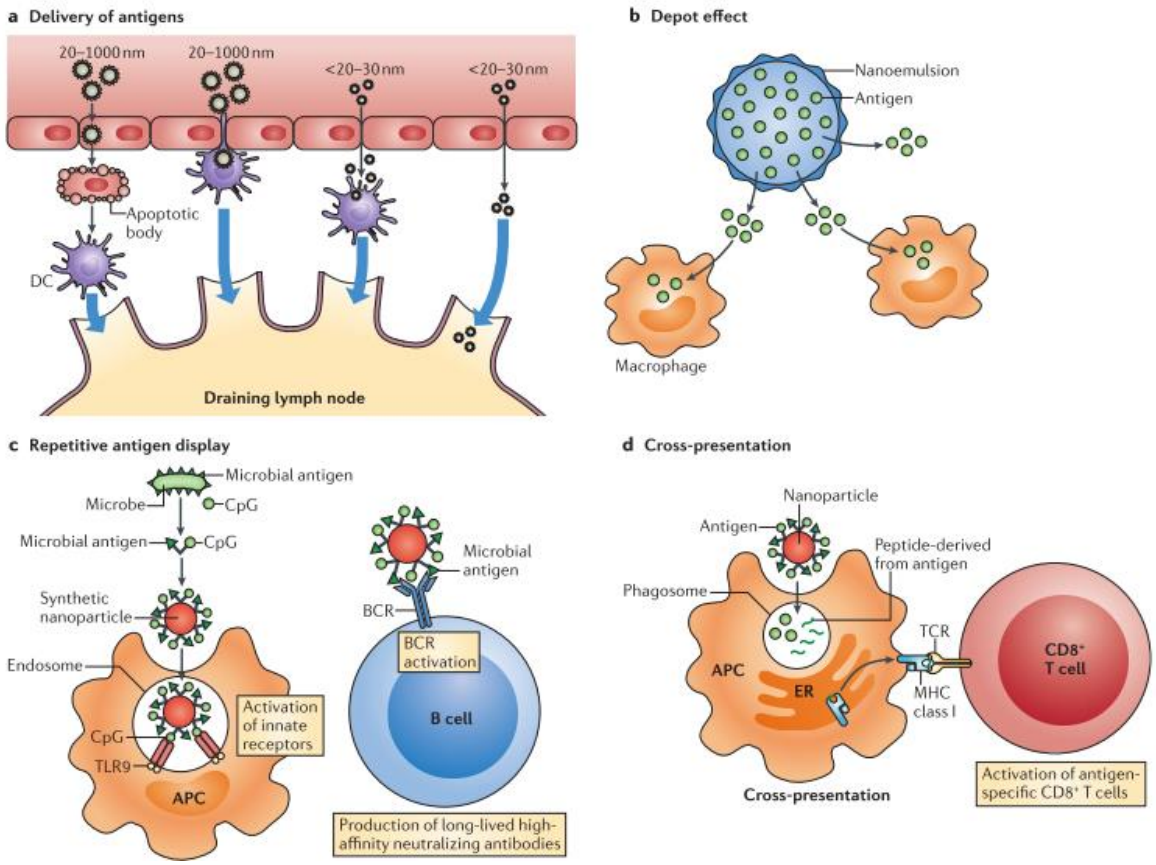

Figure 1.2. *Schematic representation of different strategies followed by nanoparticle-based vaccines in order to interact with the host immune system and shape the desired immune responses. Taken from Smith et al* [60].

Another approach commonly employed in the design of immunoactive nanoparticles is the incorporation of natural or synthetic PAMPs as adjuvants in addition to the antigen of interest. Nanoparticles deliver adjuvants into endosomal compartments of APCs, where important pattern recognition receptors (PRRs) are located. In this way, the nanoparticles are biomimetic structures

that mediate the activation of innate immune receptors, potentiating the immune responses triggered against the vaccine antigen. Next, antigen-presenting cells process and cross-present antigens to $CD8^+$ T lymphocytes through the MHC-I complex, activating adaptive immune responses. Particulate carriers increase the chances of antigens to be cross-presented compared to their soluble forms due to the targeted delivery to the lymph nodes and enhanced nanoparticle uptake by APCs. Moreover, the possibility of co-delivering antigen plus adjuvant to a unique cell enables the reduction of the doses required to elicit effective immune responses.

Finally, some materials show inherent adjuvanticity. For example, polymeric nanoparticles that contain a hydrophobic domain, such as those made of PLGA or chitosan, trigger the activation of dendritic cells *in vitro* and cellular responses *in vivo* even in the absence of additional adjuvants [67]. Iron oxide nanoparticles have recently been reported to induce a shift in the tumor microenvironment through the polarization of tumor associated macrophages (TAMs) from the M2 immunosuppressive to the M1 pro-inflammatory phenotype [68]. The self-adjuvanticity of cationic liposomes remains controversial. Some authors support the activation of DCs as a consequence of the surface charge density associated to cationic nanoparticles [69], while others demonstrate the immunogenicity of neutral or anionic particles [70].

From the biological point of view, nanoparticle-based immunotherapeutic strategies aim two main goals: the modulation of anti-tumor immunity and the regulation of the tumor microenvironment. In the first case, the objective is the generation of robust antigen-specific CTL responses to effectively recognize and eliminate tumoral cells. To tackle this, the activation of DCs has been demonstrated through a variety of strategies:

- The coupling of antigens to nanoparticles, both entrapped [71] or chemically conjugated to them [72]. The success of this strategy is based on the enhanced protection of the antigen on its way towards APC recognition. However, each approach (entrapment *vs* chemical conjugation) provides specific advantages. For instance, antigens packaged inside polymeric nanoparticles tend to present antigens to MHC-II, triggering $CD4^+$ responses, whereas $CD8^+$ T cell responses are preferentially activated upon the presentation of antigens to MHC-I by nanoparticles that carry the antigen attached to its surface [73]. In this sense, the conjugation of antigen to nanoparticles would be preferable for the development of anti-cancer vaccines since in this context cellular CTL responses

correlate with improved survival [74]. Some authors demonstrated that the progressive antigen release from polymeric nanoparticles elicits more potent cellular responses compared to other formulations that favor a burst antigen release, highlighting the importance of the kinetics of antigen release [75, 76]. In this case, the most beneficial antigen attachment strategies would be those that enable a sustained release of the antigenic material.

- The incorporation of multiple antigenic peptides to nanoparticles in order to reinforce the immunosurveillance role of the immune system [77]. Since the tumor can evade the immune recognition by presenting a myriad of mutated versions of antigens, the administration of a variety of antigenic epitopes would increase the chances of the immune system for recognizing the tumor.

- The co-administration of antigen and adjuvants to potentiate DC maturation [78]. Both the loading of antigen and adjuvant on the same or separate nanocarriers have been reported to induce specific CTL responses *in vivo* [79, 80]. The employment of particulate forms of antigen and adjuvants facilitates the targeting to the same intracellular compartment, which has been demonstrated to be crucial for obtaining efficient immune responses [81].

Apart from the modulation of anti-tumor immunity, another immunotherapeutic strategy in which nanotechnology is making an important contribution is the regulation of the tumor microenvironment. For this purpose, several approaches have been investigated:

- Suppression of the immunoinhibitory nature of the tumor microenvironment through the targeted silencing of some of the key inducers, such as the transcription factor STAT3 or the transforming growth factor β (TGFβ) [82, 83]. This strategy increases the $CD8^+$ T-cell infiltration rate into the tumor, resulting in improved outcomes.

- Modulation of the activity or proliferation of tumor infiltrating immune cellular populations that potentiate the immunosuppressive nature of the tumor microenvironment by blocking CTL responses, such as tumor-associated macrophages (TAMs) or myeloid derived suppressor cells (MDSCs). Both populations can be selectively depleted through

the targeted release of nanoparticles loaded with cytotoxic drugs such as clodronate or 6-thioguanine [84, 85]. Alternatively, the M2 immunosuppressive phenotype of TAMs can be shifted towards a M1 pro-inflammatory profile in order to reverse the tumor supportive role of this cellular population. In this case, the intrinsic immunogenic properties of iron oxide nanoparticles can be exploited [68].

Exciting advances are currently under development related to the application of biomaterials to immunotherapy [86]. An innovative example is the *de novo* generation of synthetic lymphoid organs *in vivo* [87] or the *in vitro* generation of a thymus-resembling structure that acts as a platform to create large amounts of T lymphocytes *in vitro* for supporting anti-cancer immunotherapeutic approaches such as autologous cell transfers [88]. Another impressive proposal is the design of nanomaterials-based artificial antigen presenting cells (APCs) that trigger T cell immune responses eliminating the need of autologous APCs manipulation *ex vivo*. In this case, biomaterials are loaded with the T cell growth factor IL-2, essential for the expansion and differentiation of T lymphocytes, and the anti-CD3 antibody, which activates T cells by clustering TCR-CD3 complexes on the T cell membrane [89].

All in all, nanoparticle-based therapeutic strategies are providing encouraging results in the pre-clinical stage. Nevertheless, several obstacles must be overcome in the near future before nanomaterial-enabled cancer immunotherapy is widely applicable in the clinic. For instance, more accurate animal models are required in order to predict the vaccine efficacy in humans and non-human primates. In the years to come, nanomedicine will greatly benefit from advances in oncoimmunology, which will provide a deeper understanding of immunoregulatory mechanisms, the tumor microenvironment contribution, the vaccine kinetics and the interaction between the immune system and biomaterials. From the nanomaterials point of view, safety issues must be clarified in order to avoid deleterious responses inherent to the materials themselves. The main toxicity concerns related to inorganic nanoparticles are related to the long-term persistence in the host of non-biodegradable particles, the size-dependent biodistribution, the surface charge and hydrophobicity of such materials. The safety-related requirements of a candidate vaccine may vary depending on its potential application. The administration of nanomaterials-based vaccines is more likely to occur for the treatment of patients suffering from a potentially lethal disease

such as cancer, rather than as a prophylactic treatment for children. In the latter case, the safety standard is expected to be reasonably higher than in the former one, in which some adverse side-effects might be tolerated. Ideally, nanoparticulate therapies should ensure high drug loading, a long stability in circulation and an easy scalability, which remains challenging [49]. Importantly, manufacturing strategies must be defined in order to ensure a reproducible and controlled production of high-quality nanodevices with a reasonable cost both of the manufacturing process and the final product.

1.3. Bibliography.

1. Morrissey K, Yuraszeck T, Li C-C, Zhang Y, Kasichayanula S. Immunotherapy and Novel Combinations in Oncology: Current Landscape, Challenges, and Opportunities. *Clin Transl Sci*. 2016;9(2):89-104.

2. Farkona S, Diamandis EP, Blasutig IM. Cancer immunotherapy: the beginning of the end of cancer? *BMC Med*. 2016;14:73.

3. Martin-Liberal J, Ochoa De Olza M, Hierro C, Gros A, Rodon J, Tabernero J. The expanding role of immunotherapy. *Cancer Treat Rev*. 2017;54:74-86.

4. Berraondo P, Ochoa MC, Rodriguez-Ruiz ME, Minute L, Lasarte JJ, Melero I. Immunostimulatory Monoclonal Antibodies and Immunomodulation: Harvesting the Crop. *Cancer Res*. 2016;76(10):2863-2867.

5. Nemunaitis J. Vaccines in cancer: GVAX, a GM-CSF gene vaccine. *Expert Rev Vaccines*. 2005;4(3):259-274.

6. Dowling JK, Mansell A. Toll-like receptors: the swiss army knife of immunity and vaccine development. *Clin Transl Immunol*. 2016;5(5):e85.

7. Fu J, Kanne DB, Leong M, et al. STING agonist formulated cancer vaccines can cure established tumors resistant to PD-1 blockade. *Sci Transl Med*. 2015;7(283):283ra52.

8. Meyers DE, Wang AA, Thirukkumaran CM, Morris DG. Current immunotherapeutic

strategies to enhance oncolytic virotherapy. *Front Oncol*. 2017;7:114.

9. De Munck J, Binks A, McNeish IA, Aerts JL. Oncolytic virus-induced cell death and immunity: a match made in heaven? *J Leukoc Biol*. 2017;102(3):631-643.

10. Pardoll DM. The blockade of immune checkpoints in cancer immunotherapy. *Nat Rev Cancer*. 2012;12(4):252-264.

11. Adachi K, Tamada K. Immune checkpoint blockade opens an avenue of cancer immunotherapy with a potent clinical efficacy. *Cancer Sci*. 2015;106(8):945-950.

12. Sharma P, Allison JP. The future of immune checkpoint therapy. *Science (80-).* 2015;348(6230):56-61.

13. Topalian SL, Drake CG, Pardoll DM. Immune checkpoint blockade: a common denominator approach to cancer therapy. *Cancer Cell*. 2015;27(4):450-461.

14. Radvanyi LG. Tumor-Infiltrating Lymphocyte Therapy: Addressing Prevailing Questions. *Cancer J*. 2015;21(6):450-464.

15. Constantino J, Gomes C, Falcão A, Neves BM, Cruz MT. Dendritic cell-based immunotherapy: a basic review and recent advances. *Immunol Res*. 2017;65(4):798-810.

16. Debets R, Donnadieu E, Chouaib S, Coukos G. TCR-engineered T cells to treat tumors: Seeing but not touching? *Semin Immunol*. 2016;28(1):10-21.

17. Hartmann J, Schüßler-Lenz M, Bondanza A, Buchholz CJ. Clinical development of CAR T cells—challenges and opportunities in translating innovative treatment concepts. *EMBO Mol Med*. 2017;9(9):1183-1197.

18. Huang Y, Li D, Qin D-Y, et al. Interleukin-armed chimeric antigen receptor-modified T cells for cancer immunotherapy. *Gene Ther*. 2017. doi:10.1038/gt.2017.81.

19. Piscopo NJ, Mueller KP, Das A, et al. Bioengineering solutions for manufacturing challenges in CAR T cells. *Biotechnol J*. 2017. doi:10.1002/biot.201700095.

20. FDA. Food and Drug Administration approval for Kymriah - tisagenlecleucel. 2017.

https://www.fda.gov/BiologicsBloodVaccines/CellularGeneTherapyProducts/ApprovedProducts/ucm573706.htm.

21. Yaddanapudi K, Mitchell RA, Eaton JW. Cancer vaccines. Looking to the future. *Oncoimmunology*. 2013;2(3):e23403.

22. Melero I, Gaudernack G, Gerritsen W, et al. Therapeutic vaccines for cancer: an overview of clinical trials. *Nat Rev Clin Oncol*. 2014;11(9):509-524.

23. Pilot Study of a Breast Cancer Vaccine Plus Poly-ICLC for Breast Cancer. https://clinicaltrials.gov/ct2/show/study/NCT01532960.

24. Wurz GT, Kao C-J, Wolf M, Degregorio MW. Tecemotide: An antigen-specific cancer immunotherapy. *Hum Vaccin Immunother*. 2014;10(11):3383-3393.

25. Butts C, Socinski MA, Mitchell PL, et al. Tecemotide (L-BLP25) versus placebo after chemoradiotherapy for stage III non-small-cell lung cancer (START): A randomised, double-blind, phase 3 trial. *Lancet Oncol*. 2014;15(1):59-68.

26. FDA. Food and Drug Administration approval for imiquimod - Aldara cream 5%. https://www.accessdata.fda.gov/drugsatfda_docs/label/2010/020723s022lbl.pdf.

27. Lee Y-R, Lee Y-H, Im S-A, et al. Biodegradable Nanoparticles Containing TLR3 or TLR9 Agonists Together with Antigen Enhance MHC-restricted Presentation of the Antigen. *Arch Pharm Res*. 2010;33(11):1859-1866.

28. Kasturi SP, Skountzou I, Albrecht RA, et al. Programming the magnitude and persistence of antibody responses with innate immunity. *Nature*. 2011;470(7335):543-547.

29. Siefert AL, Caplan MJ, Fahmy TM. Artificial bacterial biomimetic nanoparticles synergize pathogen- associated molecular patterns for vaccine efficacy. *Biomaterials*. 2016;97:85-96.

30. Sokolova V, Knuschke T, Kovtun A, Buer J, Epple M, Westendorf AM. The use of calcium phosphate nanoparticles encapsulating Toll-like receptor ligands and the antigen hemagglutinin to induce dendritic cell maturation and T cell activation. *Biomaterials*.

2010;31(21):5627-5633.

31. Stone GW, Barzee S, Snarsky V, et al. Nanoparticle-Delivered Multimeric Soluble CD40L DNA Combined with Toll-Like Receptor Agonists as a Treatment for Melanoma. *PLoS One*. 2009;4(10):e7334.

32. Silva JM, Zupancic E, Vandermeulen G, et al. In vivo delivery of peptides and Toll-like receptor ligands by mannose-functionalized polymeric nanoparticles induces prophylactic and therapeutic anti-tumor immune responses in a melanoma model. *J Control Release*. 2015;198:91-103.

33. Whiteside TL, Demaria S, Rodriguez-Ruiz ME, Zarour HM, Melero I. Emerging Opportunities and Challenges in Cancer Immunotherapy. *Clin Cancer Res*. 2016;22(8):1845-1855.

34. Disis ML, Gooley TA, Rinn K, et al. Generation of T-cell immunity to the HER-2/neu protein after active immunization with HER-2/neu peptide-based vaccines. *J Clin Oncol*. 2002;20(11):2624-2632.

35. Pankhurst QA, Connolly J, Jones SK, Dobson J. Applications of magnetic nanoparticles in biomedicine. *J Phys D Appl Phys*. 2003;36(3):167-181.

36. Colombo M, Carregal-Romero S, Casula MF, et al. Biological applications of magnetic nanoparticles. *Chem Soc Rev*. 2012;41(11):4306-4334.

37. Connell JJ, Patrick PS, Yu Y, Lythgoe MF, Kalber TL. Advanced cell therapies: targeting, tracking and actuation of cells with magnetic particles. *Regen Med*. 2015;10(6):757-772.

38. Safarik I, Safarikova M. Magnetic techniques for the isolation and purification of proteins and peptides. *Biomagn Res Technol*. 2004;2(1):7.

39. Gu H, Xu K, Xu C, Xu B. Biofunctional magnetic nanoparticles for protein separation and pathogen detection. *Chem Commun (Camb)*. 2006;9:941-949.

40. Borlido L, Azevedo AM, Roque ACA, Aires-Barros MR. Magnetic separations in biotechnology. *Biotechnol Adv*. 2013;31(8):1374-1385.

41. Kandasamy G, Maity D. Recent advances in superparamagnetic iron oxide nanoparticles (SPIONs) for in vitro and in vivo cancer nanotheranostics. *Int J Pharm*. 2015;496(2):191-218.

42. Estelrich J, Escribano E, Queralt J, Busquets MA. Iron Oxide Nanoparticles for Magnetically-Guided and Magnetically-Responsive Drug Delivery. *Int J Mol Sci*. 2015;16(4):8070-8101.

43. Beik J, Abed Z, Ghoreishi FS, et al. Nanotechnology in hyperthermia cancer therapy: From fundamental principles to advanced applications. *J Control Release*. 2016;235:205-221.

44. Kafrouni L, Savadogo O. Recent progress on magnetic nanoparticles for magnetic hyperthermia. *Prog Biomater*. 2016;5(3-4):147-160.

45. Mao X, Xu J, Cui H. Functional nanoparticles for magnetic resonance imaging. *Wiley Interdiscip Rev Nanomedicine Nanobiotechnology*. 2016;8(6):814-841.

46. Garcia J, Tang T, Louie AY. Nanoparticle-based multimodal PET / MRI. *Nanomedicine (Lond)*. 2015;10(8):1343-1359.

47. Jasmin, Torres de Souza G, Louzada RA, Rosado-de-Castro PH, Mendez-Otero R, Campos de Carvalho AC. Tracking stem cells with superparamagnetic iron oxide nanoparticles: perspectives and considerations. *Int J Nanomedicine*. 2017;12:779-793.

48. Korchinski DJ, Taha M, Yang R, Nathoo N, Dunn JF. Iron Oxide as an MRI Contrast Agent for Cell Tracking. *Magn Reson Insights*. 2015;8(S1):15-29.

49. Sengupta S. Cancer Nanomedicine: Lessons for Immuno-Oncology. *Trends in Cancer*. 2017;3(8):551-560.

50. Grimaldi AM, Incoronato M, Salvatore M, Soricelli A. Nanoparticle-based strategies for cancer immunotherapy and immunodiagnostics. *Nanomedicine (Lond)*. 2017. doi:10.2217/nnm-2017-0208.

51. Goldberg MS. Immunoengineering: How nanotechnology can enhance cancer

immunotherapy. *Cell*. 2015;161(2):201-204.

52. Irvine DJ, Swartz MA, Szeto GL. Engineering synthetic vaccines using cues from natural immunity. *Nat Mater*. 2013;12(11):978-990.

53. Reddy ST, Van Der Vlies AJ, Simeoni E, et al. Exploiting lymphatic transport and complement activation in nanoparticle vaccines. *Nat Biotechnol*. 2007;25(10):1159-1164.

54. Manolova V, Flace A, Bauer M, Schwarz K, Saudan P, Bachmann MF. Nanoparticles target distinct dendritic cell populations according to their size. *Eur J Immunol*. 2008;38(5):1404-1413.

55. Wilhelm S, Tavares AJ, Dai Q, et al. Analysis of nanoparticle delivery to tumours. *Nat Rev Mater*. 2016;1(5):16014.

56. Blanco MD, Teijón C, Olmo RM, Teijón JM. Targeted Nanoparticles for Cancer Therapy. *Recent Adv Nov drug Carr Syst Chapter 9*. 2012:241-278. http://www.intechopen.com/books/recent-advances-in-novel- drug-carrier-systems.

57. Alexander-Bryant AA, Vanden Berg-Foels WS, Wen X. Bioengineering Strategies for Designing Targeted Cancer Therapies. *Adv Cancer Res*. 2013;118:1-59.

58. Liu J, Yu M, Zhou C, Yang S, Ning X, Zheng J. Passive Tumor Targeting of Renal Clearable Luminescent Gold Nanoparticles: Long Tumor Retention and Fast Normal Tissue Clearance. *J Am Chem Soc*. 2013;135(13):4978-4981.

59. Dobrovolskaia MA, Aggarwal P, Hall JB, McNeil SE. Preclinical Studies To Understand Nanoparticle Interaction with the Immune System and Its Potential Effects on Nanoparticle Biodistribution. *Mol Pharm*. 2008;5(4):487-495.

60. Smith DM, Simon JK, Baker JR. Applications of nanotechnology for immunology. *Nat Rev Immunol*. 2013;13(8):592-605.

61. Gomes A, Mohsen M, Bachmann M. Harnessing Nanoparticles for Immunomodulation and Vaccines. *Vaccines*. 2017;5(1):6.

62. Leleux J, Roy K. Micro and Nanoparticle-Based Delivery Systems for Vaccine

Immunotherapy: An Immunological and Materials Perspective. *Adv Healthc Mater*. 2013;2(1):72-94.

63. Zhao L, Seth A, Wibowo N, et al. Nanoparticle vaccines. *Vaccine*. 2014;32(3):327-337.

64. The RTS S Clinical Trials Partnership. Efficacy and Safety of the RTS,S/AS01 Malaria Vaccine during 18 Months after Vaccination: A Phase 3 Randomized, Controlled Trial in Children and Young Infants at 11 African Sites. *PLOS Med*. 2014;11(7):e1001685.

65. Swartz MA, Hirosue S, Hubbell JA. Engineering approaches to immunotherapy. *Sci Transl Med*. 2012;4(148):148rv9.

66. Purwada A, Roy K, Singh A. Engineering vaccines and niches for immune modulation. *Acta Biomater*. 2014;10(4):1728-1740.

67. Park J, Babensee JE. Differential functional effects of biomaterials on dendritic cell maturation. *Acta Biomater*. 2012;8(10):3606-3617.

68. Zanganeh S, Hutter G, Spitler R, et al. Iron oxide nanoparticles inhibit tumour growth by inducing pro-inflammatory macrophage polarization in tumour tissues. *Nat Nanotechnol*. 2016;11(11):986-994.

69. Ma Y, Zhuang Y, Xie X, et al. The role of surface charge density in cationic liposome-promoted dendritic cell maturation and vaccine-induced immune responses. *Nanoscale*. 2011;3(5):2307-2314.

70. Yanasarn N, Sloat BR, Cui Z. Negatively charged liposomes show potent adjuvant activity when simply admixed with protein antigens. *Mol Pharm*. 2011;8(4):1174-1185.

71. Uto T, Wang X, Sato K, et al. Targeting of antigen to dendritic cells with poly(y-glutamic acid) nanoparticles induces antigen-specific humoral and cellular immunity. *J Immunol*. 2007;178(5):2979-2986.

72. Fifis T, Gamvrellis A, Crimeen-Irwin B, et al. Size-dependent immunogenicity: therapeutic and protective properties of nano-vaccines against tumors. *J Immunol*. 2004;173(5):3148-3154.

73. Stano A, Scott EA, Dane KY, Swartz MA, Hubbell JA. Tunable T cell immunity towards a protein antigen using polymersomes vs. solid-core nanoparticles. *Biomaterials*. 2013;34(17):4339-4346.

74. Fridman WH, Pagès F, Sautès-Fridman C, Galon J. The immune contexture in human tumours: impact on clinical outcome. *Nat Rev Cancer*. 2012;12(4):298-306.

75. Demento SL, Cui W, Criscione JM, et al. Role of sustained antigen release from nanoparticle vaccines in shaping the T cell memory phenotype. *Biomaterials*. 2012;33(19):4957-4964.

76. Johansen P, Storni T, Rettig L, et al. Antigen kinetics determines immune reactivity. *PNAS*. 2008;105(13):5189-5194.

77. Tan S, Sasada T, Bershteyn A, Yang K, Ioji T, Zhang Z. Combinational delivery of lipid-enveloped polymeric nanoparticles carrying different peptides for anti-tumor immunotherapy. *Nanomedicine*. 2014;9(5):635-647.

78. Dewitte H, Verbeke R, Breckpot K, De Smedt SC, Lentacker I. Nanoparticle design to induce tumor immunity and challenge the suppressive tumor microenvironment. *Nano Today*. 2014;9(6):743-758.

79. Schlosser E, Mueller M, Fischer S, et al. TLR ligands and antigen need to be coencapsulated into the same biodegradable microsphere for the generation of potent cytotoxic T lymphocyte responses. *Vaccine*. 2008;26(13):1626-1637.

80. Mohsen MO, Gomes AC, Cabral-miranda G, et al. Delivering adjuvants and antigens in separate nanoparticles eliminates the need of physical linkage for effective vaccination. *J Control release*. 2017;251:92-100.

81. Blander JM, Medzhitov R. Toll-dependent selection of microbial antigens for presentation by dendritic cells. *Nature*. 2006;440(7085):808-812.

82. Liao D, Liu Z, Wrasidlo WJ, et al. Targeted Therapeutic Remodeling of the Tumor Microenvironment Improves an HER-2 DNA Vaccine and Prevents Recurrence in a Murine Breast Cancer Model. *Cancer Res*. 2011;71(17):5688-5696.

83. Xu Z, Wang Y, Zhang L, Huang L. Nanoparticle-Delivered Transforming Growth Factor- β siRNA Enhances Vaccination against Advanced Melanoma by Modifying Tumor Microenvironment. *ACS Nano*. 2014;8(4):3636-3645.

84. Fritz JM, Tennis MA, Orlicky DJ, et al. Depletion of tumor-associated macrophages slows the growth of chemically induced mouse lung adenocarcinomas. *Front Immunol*. 2014;5:587.

85. Jeanbart L, Kourtis IC, Van Der Vlies AJ, Swartz MA, Hubbell JA. 6- Thioguanine- loaded polymeric micelles deplete myeloid- derived suppressor cells and enhance the efficacy of T cell immunotherapy in tumor- bearing mice. *Cancer Immunol Immunother*. 2015;64(8):1033-1046.

86. Hotaling NA, Tang L, Irvine DJ, Babensee JE. Biomaterial strategies for immunomodulation. *Annu Rev Biomed Eng*. 2015;17:317-349.

87. Suematsu S, Watanabe T. Generation of a synthetic lymphoid tissue–like organoid in mice. *Nat Biotechnol*. 2004;22(12):1539-1545.

88. Roh K-H, Roy K. Engineering approaches for regeneration of T lymphopoiesis. *Biomater Res*. 2016;20:20.

89. Steenblock ER, Fadel T, Labowsky M, Pober JS, Fahmy TM. An Artificial Antigen-presenting Cell with Paracrine Delivery of IL-2 Impacts the Magnitude and Direction of the T Cell Response. *J Biol Chem*. 2011;286(40):34883-34892.

Experimental section

ES1. Synthesis and characterization of SPION and ZnSPION.

Hydrophobic magnetite (Fe_3O_4) nanoparticles (SPION) were synthesized by the thermal decomposition method. The chemical reactants, iron(III) acetylacetonate (2 mmol), 1,2- hexadecanediol (10 mmol), oleic acid (6 mmol), oleylamine (6 mmol) and benzyl ether (20 mL), are mixed under a flow of nitrogen and heated for 210 °C for 2 h. Then the mixture is heated to reflux (300 °C) for 1 h. After cooling down to room temperature, ethanol (40 mL) is added to precipitate nanoparticles and they are separated by centrifugation (30 min, 3000 x g). The isolated pellet is then dissolved in hexane (10 mL) in the presence of oleic acid (0.05 mL) and oleylamine (0.05 mL). Centrifugation (10 min, 3803 x g) is applied to remove any undispersed residue. Ethanol (20 mL) is added and then centrifuged (10 min, 3803 x g).

The hydrophobic zinc ferrite nanoparticles, $(Zn_xFe_{1-x})Fe_2O_4$ ($x<=0.4$) (ZnSPION) were prepared by the thermal decomposition method by heating at 200°C a mixture of iron(III) acetylacetonate (4 mmol), hexadecanediol (25 mmol), oleic acid (15 mmol), hexadecylamine (15 mmol) and octyl ether for 1 h. During the second step of the reaction, diethylzinc (0.85 mmol) is added as a Zn source, and the temperature of the reaction is raised up to 300 °C for 1 h. Then the mixture is cooled down to room temperature, and ethanol (40 mL) is added to precipitate nanoparticles. For further purification, the pellet is centrifuged (10 min, 3803 x g) and left on air until complete evaporation.

The synthesis of hydrophobic iron oxide nanoparticles was carried out by Dr. Macarena Cobaleda and Dr. Nina Gómez.

The size of hydrophobic IONPs was determined by transmission electron microscopy (TEM) on a JEOL JEM-2011 electron microscope operating at 200kV. The samples were prepared by depositing a drop of IONPs onto a copper specimen grid coated with a holey carbon film (*Electron Microscopy Sciences*). Samples were prepared by dissolving 1 mg of nanoparticles in tetrahydrofuran (THF) to a final concentration of 0.1 mg/mL. At least 300 particles were measured using the Image J software to determine IONP size.

ES2. Synthesis and characterization of SPION and ZnSPION- filled micelles.

The synthesis of the water soluble IONPs-filled micelles is based on the self-assembly of PEGylated phospholipids around the hydrophobic cores of IONPs.

The synthesis of SPION filled micelles was carried out by dissolving DPPE-mPEG(2000) (2 mg) and SPION (1 mg) in chloroform (500 µL). The solvent was allowed to evaporate overnight in a 3 mL round bottom flask at RT. Any remaining solvent was removed under vacuum for 1 h. The flask was placed in a water bath at 80 °C for 30 s, after which 1 mL of nanopure water was added. The solution was transferred to an Eppendorf tube and centrifuged at 9700 g for 5 min. The pellet was discarded and the supernatant was passed through a 0.45 µm filter. This solution was ultracentrifuged (369 000 x g, 1 h, 3 cycles) to remove the empty micelles. Finally the pellet was dissolved in 1 mL of nanopure water.

For the synthesis of ZnSPION-filled micelles, different ratios of lipids and ZnSPION-to-lipid ratios were used: zinc ferrite nanoparticles (1 mg) and DPPE-mPEG(2000) (5 mg) for ZnSPION-PEG or DOTAP (1 mg) and DPPE-mPEG(2000) (4 mg) for ZnSPION-DOTAP were dissolved in chloroform (500 µL). The rest of the protocol was followed as previously described.

Fluorescent micelles were prepared following the same protocol described above, with only two modifications: lissamine rhodamine dipalmitoylphosphatidylethanolamine was added (5 % of total moles of lipids) to the chloroform solutions of PEGylated lipids and IONPs; and the whole protocol was carried out in the darkness to preserve the fluorescence of the dye.

The hydrodynamic size of micelles and zeta potential in solution was measured with a NanoSizer (Malvern Nano-Zs, UK). Size measurements were carried out in disposable micro cuvettes (70 µL, *Brand*), with samples diluted in water to a final iron concentration of 8 mM, while zeta-potential measurements were acquired in clear disposable folded capillary cells (*Malvern*) with samples diluted in nanopure water with NaCl 0.09% V/V to a final concentration of 1 mM Fe. The selected voltage was 40 V. All the results are an average of 5 measurements matching quality criteria.

TEM studies were conducted on a JEOL JEM-2011 electron microscope operating at 200 kV. The samples were prepared by depositing a drop of IONPs onto a copper specimen grid coated

with a holey carbon film (*Electron Microscopy Sciences*) after treating it to make it highly hydrophilic and allowing it to dry.

XPS experiments were performed in a SPECS Sage HR 100 spectrometer with a non-monochromatic X-ray source (aluminum Kα line of 1486.6 eV energy and 350 W). The samples were placed perpendicular to the analyzer axis and calibrated using the $3d_{5/2}$ line of Ag with a full width at half maximum (FWHM) of 1.1 eV. The selected resolution for the spectra was 10 eV of Pass Energy and 0.15 eV/step. Measurements were made in an ultra high vacuum (UHV) chamber at a pressure below $8 \cdot 10^{-8}$ mbar. XPS experiments and subsequent data analysis were carried out by Dr. Luis Yate, head of the surface analysis and fabrication platform of CIC biomaGUNE.

The thermogravimetric analysis (TGA) was performed on a TGA/SDTA 851 Mettler Toledo thermogravimetric analyzer under nitrogen atmosphere at a heating rate of 10 K/min at the SGIker analytical facility of the University of the Basque Country (UPV/EHU; San Sebastián, Spain).

Magnetic measurements were done using the Vibrating Sample Magnetometry (VSM) technique at the SGIker analytical facility of the University of the Basque Country (UPV/EHU; Leioa, Spain)). The hysteresis loops at RT, with very good low field accuracy (better than 1×10^{-5} T) were performed in a home- made VSM equipped with an electromagnet up to a maximum field of 1.8 T. Another VSM fitted to a Cryogenic Free 14 T magnet system (Cryogenic Ltd) was used for the measurements below RT from - 8 T to +8 T.

Attachment of Poly(I:C) and imiquimod. Lyophilized Poly(I:C) and imiquimod (*Invivogen*) were resuspended in endotoxin-free water to a final concentration of 1000 µg/mL and 500 µg/mL, respectively. Double-functionalized IONPs were developed through a two-step process. First, IONP-filled micelles were mixed with Poly(I:C) and the mixture was stirred overnight at 700 rpm at room temperature. The excess of unbound Poly(I:C) was purified in three cycles (5 minutes at 1475 x g) of ultrafiltration with NanoSep 100k (MWCO 100 kDa) centrifugal devices (*Pall Life Sciences*). Then, Poly(I:C)-IONP micelles were resuspended in an imiquimod solution, keeping the final volume constant (IONPs pIC→R). This mixture was stirred and purificated again exactly the same way as described above. The final pellet was resuspended in the same

initial volume of nanopure water or phosphate buffered saline (PBS) and stored at 4 °C. The same procedure with the opposite order of addition of TLR agonists was followed to develop IONPs R→pIC.

Attachment of ovalbumin. SPION-filled micelles for OVA attachment were formulated with 1 mg of SPION, 2 mg of DPPE-mPEG(2000) and 2 mg of DPPE-cPEG(2000). For the chemical activation of carboxylic groups of PEGylated lipids of SPION-filled micelles, these were mixed with EDC/NHS in 1:25:25 molar ratio and stirred for 2 h at room temperature in MES buffer 10 mM pH=5.0. The excess of EDC/NHS was removed by ultrafiltration with NanoSep 100k (MWCO 100 kDa) centrifugal devices (*Pall Life Sciences*) (1475 x g for 5 min, 3 cycles). The resulting activated SPION-micelles were resuspended in the initial volume and stirred overnight at room temperature with EndoGrade® endotoxin-free ovalbumin (*Hyglos*) in a final volume of 300 µL of phosphate buffered saline (PBS). The unbound OVA was eliminated by ultrafiltration at 1475 x g for 5 min (3 cycles). The pellet was resuspended in the initial volume of PBS (10 mM) and stored at 4 °C.

ES3. Characterization of Poly(I:C)-imiquimod-IONP micelles.

The Fe and Zn concentration in the samples were determined by ICP-OES analysis carried out by the SGIker analytical facility of the University of the Basque Country (UPV/EHU; Leioa, Spain). The samples were analyzed for Fe and Zn by ICP-OES using a Perkin Elmer Optima 5300 DV, employing an RF forward power of 1400 W, with argon gas flows of 15, 0.2 and 0.75 L/min for plasma, auxiliary and nebulizer flows, respectively. Using a peristaltic pump, sample solutions were taken up into a Gen Tip cross-Flow nebulizer and Scotts spray chamber at a rate of 1.50 mL/min. The instrument was operated in axial mode. The selected wavelengths (238.024, 239.562, 259.939 nm) were analyzed in fully quant mode (three points per unit wavelength). A range of calibration standards were prepared using single element 1000 mg/L stock solutions (*Fisher Scientific UK LTD*) and a Merck multi element standard (ICP Multi element standard solution VI CertiPUR®) was employed as a reference standard.

The quantification of bound imiquimod was performed by UV-vis spectroscopy, analyzing the absorption peak at 325 nm. The concentration of imiquimod was calculated by extrapolating that

absorbance to a calibration curve. Similarly, the Poly(I:C) content was determined by analyzing the absorption peak at 260 nm. UV-Vis absorption spectra were acquired using a NanoDrop ND 1000 (version 3.5.2) Spectrophotometer (*NanoDrop Technologies*).

The amount of OVA bound to SPION-OVA micelles was quantified using a bicinchoninic acid (BCA) protein assay reagent kit (*Thermo scientific*), after absorbance subtraction of the same concentration of parental SPION micelles. The absorbance measurements were performed in a 96-well plate with a TECAN Genios Pro 96/384 microplate reader.

Fluorescence experiments to assess the interaction of imiquimod with Poly(I:C) were conducted in a fluorometer Horiba by irradiating the samples with an excitation wavelength of 250 nm.

The interaction between Poly(I:C) and imiquimod was also determined by circular dichroism (CD) measurements. The CD spectra were acquired between 180 and 350 nm on a Jasco J-815 CD spectrometer fused with nitrogen gas. A fixed concentration of Poly(I:C) (50 μg/mL) was titrated with increasing concentrations of imiquimod until saturation was achieved. All the spectra measurements were carried out in a 1 mm path length cuvette. Results are the average of five spectra measured at room temperature. Baseline and smoothing corrections have been applied.

ES4. Imaging studies.

C57BL/6 female mice (6-8 weeks old) were s.c. challenged with $3x10^5$ B16F10(OVA) tumor cells resuspended in 100 μL of PBS. Mycoplasma test (*Lonza*) was carried out prior to injection to ensure that cells were free of contamination. The tumors were left to settle and grow until the diameter reached around 7 - 12 mm for MR imaging acquisition. At the beginning of the experiments, mice were immunized with SPION and ZnSPION decorated with Poly(I:C) and imiquimod at a concentration of 6 or 11 mMFe. 100 μL of sample were s.c. injected in the tumor vicinity. Images were acquired at times prior injection, 24 h and 48h post injection (p.i.) to analyze accumulation of nanoparticles in the inguinal lymph nodes and tumor (**Figure ES1**). Animals were anesthetized prior to imaging using 3.5 % isofluorane and maintained at 1.5 – 2.5 % isoflurane in 100 % O2 during the whole acquisition. Animals were placed in a mouse holder compatible with the MRI equipment and kept at a constant body temperature of 37 °C

throughout the study using a heated water blanket. Temperature and respiration rate was monitored with an MRI compatible animal monitoring system (SA Instruments Inc., New York, USA) with animals maintained at a respiration rate of 60 - 80 breaths per minute. Experiments were performed on a 70/30 Bruker Biospec system (Bruker Biospin GmbH, Ettlingen, Germany) using the BGA12-S mini imaging gradient and 40 mm inner diameter transmit/receive mouse body volumetric coil. Axial gradient echo experiments were performed with the following parameters: A respiration synchronized (TR = one respiration cycle) FLASH sequence, TE = 3 ms, FOV = 28 mm x 28 mm, Matrix = 256 x 256, Slice Thickness = 0.75 mm , N Slices= 32 and 2 averages. Axial T2 maps were acquired using the following parameters: A respiration synchronized (TR = 6 respiration cycles) Multi Slice Multi Echo (MSME) sequence, TE = 8, 16, 24, 32, 40, 48, 56, 64 ms; FOV = 28 mm x 28 mm, Matrix = 128 x 128, Slice Thickness = 0.75 mm, N Slices= 9 and 2 averages. The images were fitted into Levenberg-Margardt method to calculate T2 values using Bruker's Paravision 5.1 software. These experiments were carried out by Dr. Daniel Padro, head of the NMR platform of CIC biomaGUNE.

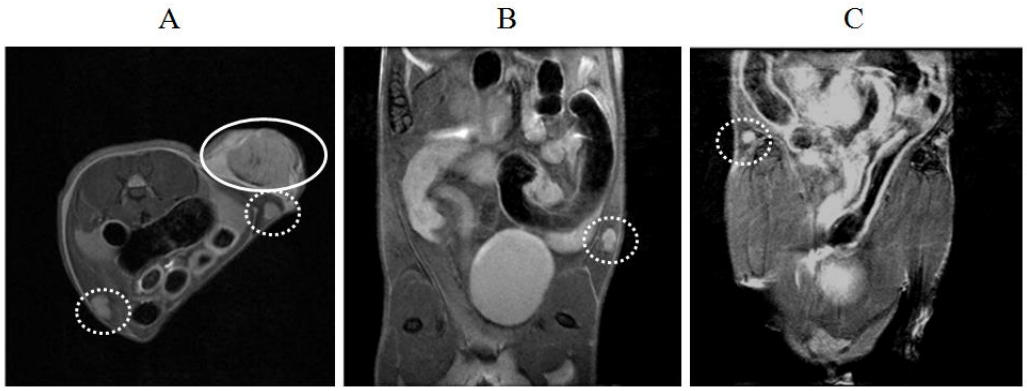

Figure ES1. *MR images of a B16F10(OVA) tumor bearing mice. Inguinal lymph nodes (dashed circles) and tumor (solid circle) are indicated on the images. Transverse (a) and longitudinal (b, c) sections are shown. Right (b) and left (c) inguinal lymph nodes are depicted separately in the longitudinal axis.*

Relaxivity measurements were carried out at 37 ºC on a Bruker Minispec mq60 instrument operating at 1.47 T. T_1 and T_2 values were measured for each sample at different Fe concentrations using inversion-recovery and CPMG methods respectively. The relaxivity values,

r_1 and r_2, were calculated through linear least squares fitting of 1/relaxation time (s^{-1}) *versus* the iron concentration ([Fe] mM). The measurements were carried out in collaboration with Dr. Nina Gómez.

The MRI phantom experiments were carried out on a Bruker Biospec 11.7 T with a 9 cm gradient capable of delivering 740 mT/m using a 40 mm volume coil. T2 maps were acquired by using Bruker's MSME (Multi slice Spin echo) sequence. The echo time (TE) values were varied in 128 steps ranging from 10 ms to 1280 ms and a repetition time (TR) of 15 s. T1 maps were obtained by using a spin echo sequence. Images were acquired at ten different TR values 150, 500, 1000, 1500, 2200, 3000, 4000, 5200, 7.600, 17500 ms). All data were acquired with: 256 x 256 points and a Field of View of 3 cm x 3 cm, slice thickness of 1.5 mm, no gap between slices and one average. T2 weighted images correspond to TE = 36 ms and TR = 15 s. The T1 and T2 map images were calculated using the Bruker's Paravision 5.1 software via the Levenberg- Margardt method. The relaxivity values, *r*1 and *r*2, were calculated through linear least squares fitting of 1/relaxation time (s- 1) versus the iron concentration ([Fe] mM). This experiment was carried out by Dr. Nina Gómez in collaboration with the NMR platform of CIC biomaGUNE.

SPECT/CT studies.

^{67}Ga was purchased as citrate solution from Molypharma (Spain) (specific activity =1.4 TBq/μmol), and converted into $^{67}GaCl_3$. Briefly, the gallium citrate solution was passed through a light silica column cartridge (Sep-Pak, Waters) to selectively retain the radiometal. The cartridge was washed with ultrapure water (10 mL) and ^{67}Ga was finally eluted with HCl 0.1 M solution. The eluate was collected in different 100 μL fractions, and only those containing the maximum activity concentration were used in subsequent labeling experiments. The eluted ^{67}Ga chloride solution (100 μL, c.a. 110 MBq) was then mixed with 100 μL of IONP micelle solution and diluted up to final volume of 400 μL in acetate buffer (pH = 3.8 ± 0.1). After incubation at 70 °C during 30 min, the reaction crude was cooled down to room temperature and the labeled NPs were separated via centrifugal filtration (6708 x g for 10 min for SPION pIC->R; 3354 x g for 10 min for ZnSPION pIC->R) using AmiconUltracel 100k (MWCO 100 kDa) centrifugal devices (*Merck*), and washed twice with phosphate buffered solution. The retentate was

recovered from the filter by the addition of 10 mM PBS (100 μL). The total radioactivity in the filtrates and retentates were measured in a CRC-25R dose calibrator (*Capintec*, USA) in order to determine the incorporation efficiency. For stability studies, one batch of ^{67}Ga-IONP micelles was fractioned in different aliquots, which were incubated in the presence of DOTA chelating agent (c.a. 10^6 moles of DOTA per mole of nanoparticle) at 37 °C. At different timepoints, the samples were filtered in order to separate the NPs from the ^{67}Ga complexed to DOTA, and radioactivity in the retentate and in the filtrate was measured with the CRC-25R dose calibrator (*Capintec*, USA). The dissociation of ^{67}Ga (expressed in percentage) from the radiolabeled micelles at each time point was calculated as the ratio between the amount of radioactivity in the filter and the starting amount of radioactivity.

C57BL/6 female mice (6-8 weeks old) were s.c. challenged with $3x10^5$ B16F10(OVA) tumor cells resuspended in 100 μL of PBS. Mycoplasma test (*Lonza*) was carried out prior to injection to ensure that cells were free of contamination. The tumors were left to settle and grow until the diameter reached around 7 - 12 mm. Then, mice were immunized with ^{67}Ga labeled SPION and ZnSPION filled micelles decorated with Poly(I:C) and imiquimod dissolved in PBS to a concentration of 1.21 mMFe. 50 μL of sample/mouse were s.c. injected in the tumor vicinity. Animals were anesthetized prior to imaging using 3.5 % isofluorane and maintained at 1.5 – 2.5 % isoflurane in 100 % O2 during the whole acquisition. Whole-body SPECT/CT scans were acquired at 3 and 24 h postinjection (p.i.). With the full ring detector, 360° of data were acquired by rotating the collimator 45° (45 steps, 1°/step). Data were collected in an energy acquisition window from 125−150 keV to 84−102 keV and acquisition times from 60 min (80 s/step) to 45 min (60 s/step). At the end of the scanning procedure, the mice were culled by cervical dislocation and organs of interest removed. Analysis of the injected dose percentage per organ was performed by measuring their activity with a WIZARD22470 Automatic Gamma Counter (*PerkinElmer*). These experiments were carried out by Dr. Ane Ruiz de Angulo in collaboration with the radiochemistry platform of CIC biomaGUNE.

ES5. Cytotoxicity studies.

J774.A1 murine macrophage cell line was purchased from the ATCC and cultured in DMEM (*Gibco, Life Technologies*) supplemented with 10 % FBS (*Gibco, Life Technologies*), 1 % L-

glutamine (*Gibco, Life Technologies*) and 1% penicillin-streptomycin (*Sigma Aldrich*), and maintained in a humid atmosphere at 37 °C and 5 % CO_2. To assess cell viability at 24 h, cells were seeded at 2.5 x 10^4 cells/well (100 µL per well) in flat bottom 96-well plates and allowed to adhere overnight.

The B16F10(OVA) murine skin melanoma cell line stably transfected with a plasmid responsible of the expression of ovalbumin was kindly gifted by the group of Dr. Pablo Sarobe (Center of Applied Medical Research, CIMA, Pamplona, Spain). These cells were cultured in RPMI (*Lonza*) supplemented with 10 % FBS, 1 % L-glutamine and 1% penicillin-streptomycin, and maintained in a humid atmosphere at 37 °C and 5 % CO_2. To assess cell viability at 24, 48 and 72 h, cells were seeded at 7 x 10^3, 2.5 x 10^3 and 1.5 x 10^3 cells/well (100 µL/well), respectively, in flat bottom 96-well plates and allowed to adhere overnight.

Media was removed from each well prior to adding 100 µL of each sample, properly diluted in cell culture media, per well in triplicate. After incubation, the supernatants were removed and frozen for further cytokine analysis. To determine cell viability, 100 µL/well of MTT reagent (*Roche*) diluted in media to a final concentration of 0.25 mg/mL was added after removal of the supernatant. After a 1 h-incubation at 37 °C, the reagent was removed and 200 µL/well of DMSO were added to solubilize formazan crystals. Finally the optical density of the samples was measured in a TECAN Genios Pro 96/384 microplate reader at 550 nm and data was represented as the percentage of cell survival compared to control wells.

ES6. *In vitro* co-culture assays.

In order to determine the production of the M1 macrophage phenotype marker TNFα, the J774A.1 macrophage cell line was co-cultured with the B16F10(OVA) melanoma cell line in dual chamber transwell systems with 8 µm-sized microporous polycarbonate membranes (*Corning*). 5x10^4 J774A.1 cells/well were seeded onto the upper chambers of the transwell plates, and 7x10^3 B16F10(OVA) cells/well were placed into the bottom wells. Co-cultures were incubated for 24 h in a humid atmosphere at 37 °C and 5 % CO_2 with samples conveniently diluted in DMEM supplemented with 10 % FBS, 1 % L-glutamine and 1% penicillin-

streptomycin. Cell culture supernatants were collected and stored at -20 °C for further cytokine content analysis by ELISA.

ES7. Quantification of cytokines and antibody production by ELISA.

IL-6, IL-12, IL-10 and TNFα were measured in cell supernatants using sandwich ELISA following the manufacturer's instructions (murine IL-6 mini EDK ELISA kit, *R&D Systems*; murine IL-12 and TNFα mini EDK ELISA kits, *Peprotech;* mouse IL-10 ELISA MAX standard set, *Biolegend*). A 4-parameter sigmoidal (logistic) standard curve was used to quantify cytokines (GraphPad Prism 5 software). Results are expressed as mean ± SEM in pg/mL or ng/mL.

Anti-OVA IgG1, IgG2c and IgGt antibodies were measured in blood serum using indirect ELISA. Flat bottom 96 well EIA/RIA plates (*Corning*) were covered with 50 µL/well of OVA diluted in PBS to a final concentration of 0.04 mg/mL. The samples of blood serum were obtained from immunized mice by facial vein puncture and centrifuged at 13000 x g for 5 min to remove the cellular content of the blood. After the samples incubation, the concentrations of antigen-specific antibodies were determined with HRP-conjugated anti-mouse IgG1, IgG2c and IgGt antibodies (*BioRad*) diluted 1:4000, 1:10000 and 1:500 in PBS, respectively. The results were expressed as the $\log_{10}$ value of the reciprocal of the endpoint dilution which gave an optical density (O.D.) of 0.2 or above, after the subtraction of the background levels.

In both ELISA types, the measurement of each sample was conducted in duplicate. Absorbance measurements were carried out in a TECAN Genios Pro 96/384 microplate reader at 450-550 nm.

ES8. Localization of intracellular nanoparticles by confocal microscopy.

The murine macrophage cell line J744.A1 was seeded in poly-lysine-coated 35 mm glass bottom dishes (*MatTek*) and grown at 37 ºC and 5% CO_2 in 2mL of DMEM medium supplemented with 10% bovine fetal serum, 2 mM L-glutamine, and 50 U/mL penicillin/streptomycin. Then, cells

were incubated for 1h at 37 ºC and 5 % CO_2 in media containing rhodamine-labeled ZnSPION-filled micelles (25 nM NP) with/without DOTAP decorated with Poly(I:C) and imiquimod, 1 µM LysoTracker Green DND-26 (*Invitrogen*) and 3 drops of NucRed® Live 647 ReadyProbes® Reagent (*Life Technologies*). Imaging was performed on a Zeiss LSM 510 META confocal microscope equipped with 63X magnification oil lens. Fluorescence images were taken in sequential mode at the excitation wavelengths of 488 nm, 561 nm and 633 nm for LysoTracker Green DND-26, rhodamine B or NucRed® Live 647 ReadyProbes® Reagent, respectively. The thickness of each optical slice was set at 3 µm for each color channel. Transmitted light images were also acquired. Image analysis was performed with the Zeiss LSM Image Browser. These experiments were carried out by Dr. Blanca Arnáiz.

ES9. BMDC maturation assay.

Balb/c mice (6-12 weeks old) were sacrificed by cervical dislocation and intact femurs were removed aseptically. Femurs were placed in ethanol for 2 min and washed in cold PBS. Bone marrow was flushed into cold PBS using a syringe and cellular clusters were disaggregated to obtain a homogeneous cell suspension. Erythrocytes were lysed with BD Pharm Lyse lysing buffer (*BD Biosciences*) and cells counted. 2 x 10^6 cells/dish were plated in bacterial grade Petri dishes, in 10 mL/dish of RPMI supplemented with penicillin/streptomycin (100 µg/mL), L-glutamine (2 mM), heat-inactivated FBS (10%) and GM-CSF (*Peprotech*, 20 ng/mL). On day 3, 10 mL of complete RPMI containing GM-CSF (20 ng/mL) was added to each Petri dish. On day 6, 10 mL of media was carefully removed and replaced with 10 mL/dish of fresh RPMI supplemented with GM-CSF (10 ng/mL). On day 8, BMDCs were removed by carefully dislodging semi-adherent cells using light pipetting to avoid activating the cells.

For cytotoxicity assays, cells were counted and resuspended in RPMI at a final concentration of 2 x 10^5 cells/well in 96-well tissue culture plates (100 µL/well). Samples to be tested (100 µL/well, appropriately diluted in RPMI) were added to the DC containing wells and incubated for 24 h in a humid atmosphere at 37 °C and 5 % CO_2, following which supernatants were recovered and frozen for later testing of cytokines. The cell viability of BMDCs was analysed using the MTT assay, following the same procedure described above.

For maturation assays, BMDCs were counted and resuspended in RPMI (10 % FBS, 1 % L-glutamine, 1 % penicillin-streptomycin). They were seeded in a 96-well tissue culture plate at 2 x 10^5 cells/well (100 µL/well). Samples to be tested (100 µL/well, appropriately diluted in RPMI) were added to the DC containing wells and incubated for 24 h in a humid atmosphere at 37 °C and 5 % CO_2, after which they were immunostained to analyze the expression profile of MHC-II and the maturation markers CD80, CD86 and CCR7.

To carry out the immunostaining procedure, BMDCs were firstly washed with PBS. In order to avoid non-specific cell staining, Fc receptors were blocked by incubating the cells with rat IgG2bk anti-mouse CD16/CD32 antibody (*BD Biosciences*) for 10 min at 4 °C. $CCR7^+$ cells were stained with BV421-rat IgG2ak anti-mouse CD197 (*Biolegend*) for 15 min at 37 °C. A BV421-rat IgG2ak isotype control antibody was used to establish the background level of non-specific fluorescence associated with cells after being stained with fluorochrome-associated antibodies. The next step consisted on staining cells with antibodies that define DC phenotype (APC-hamster IgG1λ2 anti-mouse CD11c and PerCP-Cy5.5-rat IgG2bk anti-mouse I-A/I-E antibodies, *Biolegend*) and maturation marker antibodies (FITC-dog IgG anti-mouse CD80 and PE-rat IgG2ak anti-mouse CD86 antibodies, *Biolegend*). The corresponding isotypes were acquired using FITC-armenian hamster IgG1 isotype control and PE-mouse IgG1 isotype control antibodies (*Biolegend*). This step was carried out at 4 °C for 15 min. Finally, cells were washed with PBS and resuspended in 200 µL of FACS buffer to be analyzed by flow cytometry using a FACS Canto II flow cytometer. The maturation markers expression was analyzed in the final gated DC population ($cd11c^+$ $MHC\text{-}II^+$). Isotype controls were included in each assay and are not included in the figures for clarity purposes. The gating strategy is detailed in **Figure ES2**.

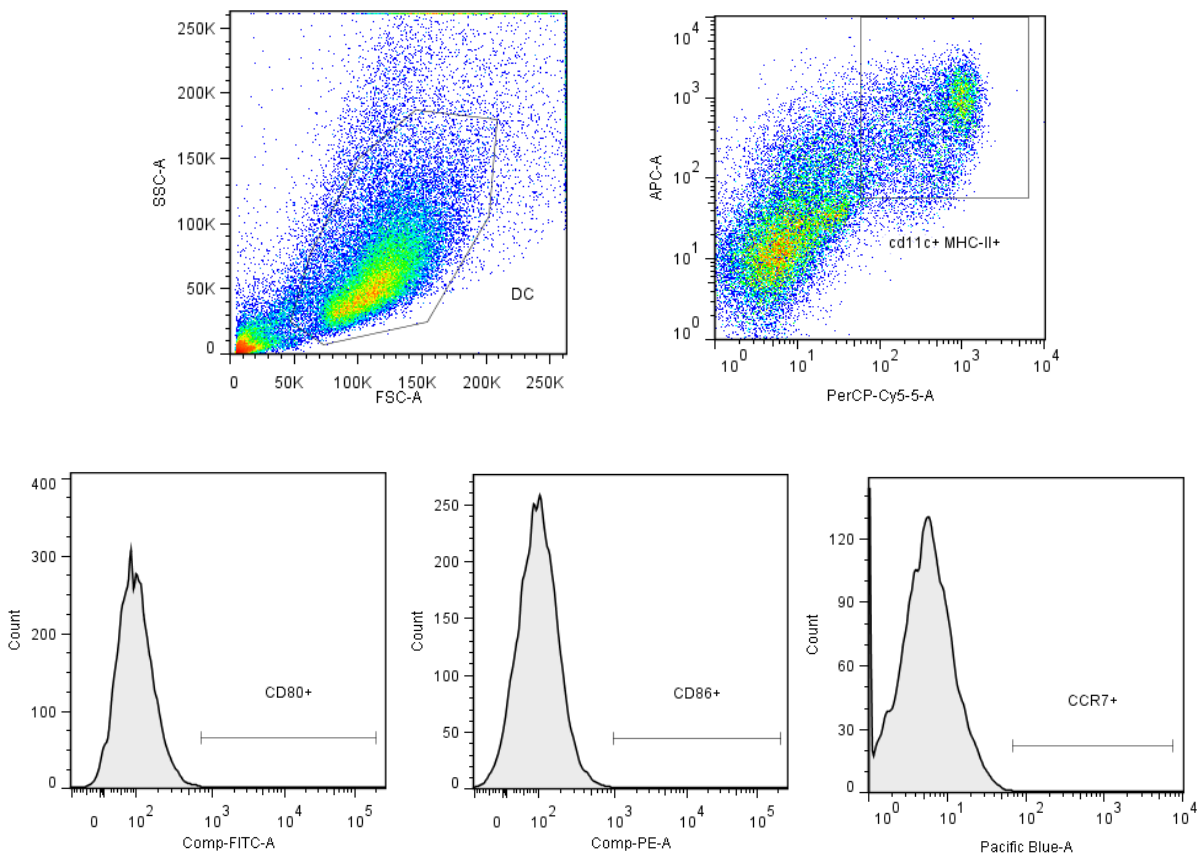

Figure ES2. *Gating strategy followed in BMCD maturation assays. The expression of maturation markers CD80, CD86 and CCR7 was analyzed in a population of dendritic cells phenotypically defined as cd11c$^+$ MHC-II$^+$.*

ES10. Animals.

Animals were cared for and handled in compliance with the Guidelines for Accommodation and Care of Animals (European Convention for the Protection of Vertebrate Animals Used for Experimental and Other Scientific Purposes) and internal guidelines, and all the experimental procedures were approved by the appropriate local authorities. All animals were housed in ventilated cages and fed on a standard diet *ad libitum*.

ES11. Splenocytes and lymphocytes primary culture preparation.

For the analysis of innate and adaptive immune responses induced *in vivo* after immunization, spleens and draining lymph nodes (dLNs) were removed and processed for further analysis *ex vivo*. Briefly, organs were perfused with tissue dissociating mix (3 mL of collagenase/DNase I diluted in RPMI media), cutted into small pieces (spleen) and incubated for 30 min at 37 °C in a sterile Petri dish. The reaction was stopped with 500 mM EDTA and organs were smashed with the plunger of a syringe. Red blood cells lysis was performed in those cell suspensions derived from spleens, by adding 1 mL of BD Pharm Lyse erythrocytes lysing buffer (*BD Biosciences*) for 1 min and rapidly quenched with 10 mL of cold PBS. The resulting cell suspensions were recollected into 15 mL tubes, washed twice with cold PBS and resuspended in complete RPMI, ready for the subsequent studies.

ES12. Assessing innate immune responses *in vivo*.

C57BL/6J mice (6-8 weeks old) were injected intra-hook in the inner side of one of the back feet with the corresponding formulations diluted in PBS (40 µL/mouse). Mice were immunized once with 2.8 µg Poly(I:C)/mouse, 0.9 µg imiquimod/mouse and 4.8 µg ZnSPION/mouse (ZnSPION pIC->R) or 5 µg Poly(I:C)/mouse, 1 µg imiquimod/mouse and 6.4 µg ZnSPION/mouse (ZnSPION-DOTAP pIC->R). An additional control with free TLR agonists at high concentration was also included in order to compare the effect of the dose on the induction of innate immune responses (12 µg Poly(I:C)/mouse and 3 µg imiquimod/mouse). 24 h after immunization, mice were sacrificed by cervical dislocation and spleen and inguinal and popliteal lymph nodes were extracted and processed as described before for further analysis of the maturation of DC and NK cellular populations. Briefly, $1x10^6$ cells/well diluted in RPMI were seeded in a 96-well plate and divided into two different staining panels. For the DC maturation analysis, cells were stained and gated as described in the *in vitro* BMDC maturation assays (**Figure ES3**), analyzing this time an additional maturation marker, CD40 (PE/Cy7-rat IgG2ak anti-mouse CD40, and its corresponding isotype control antibody PE/Cy7-rat IgG2ak, *Biolegend*).

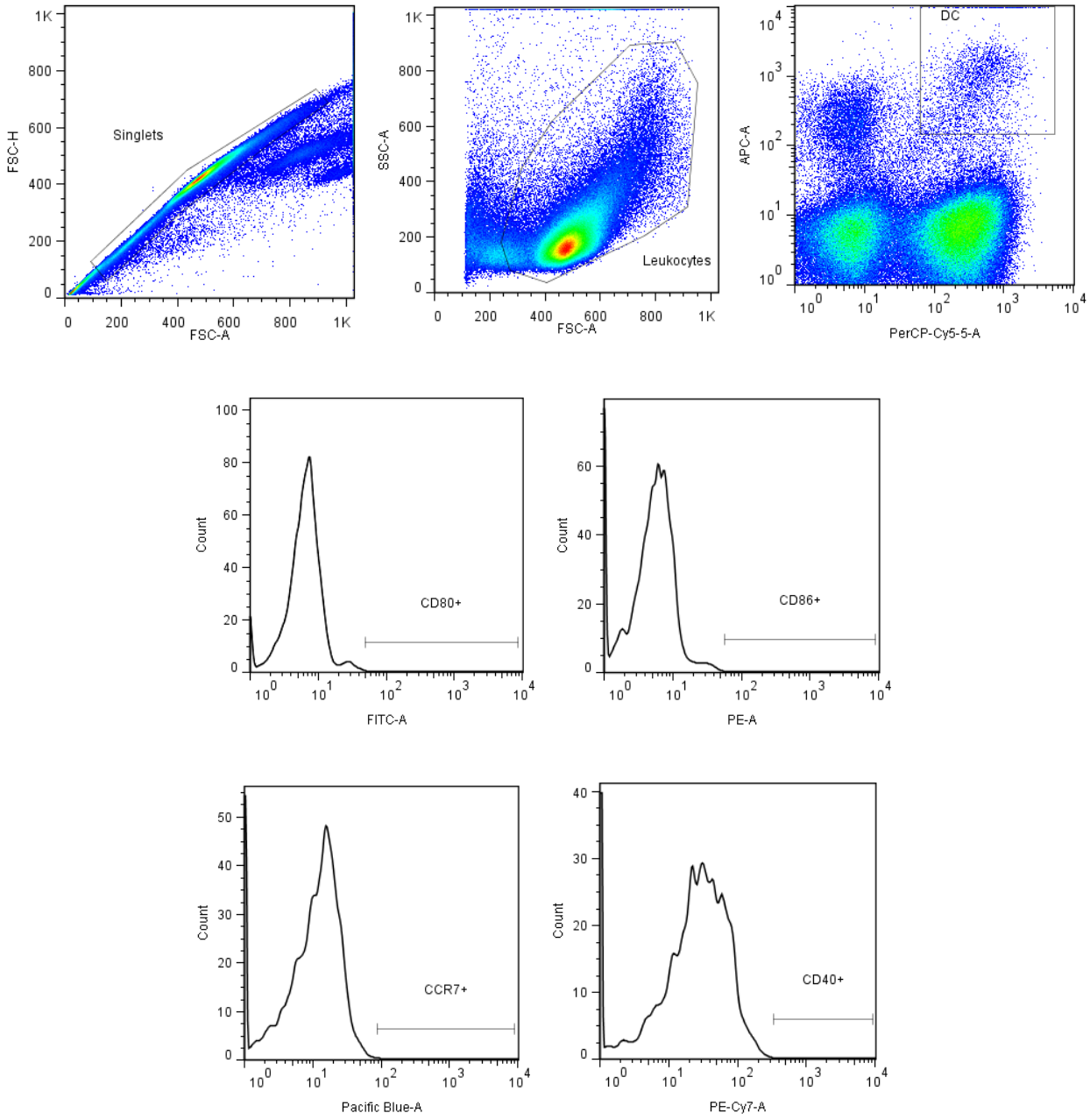

Figure ES3. *Gating strategy followed in the innate immune response assays. The expression of the maturation markers CD80, CD86, CD40 and CCR7 was analyzed in a population of dendritic cells phenotypically defined as cd11c^{+} MHC-II^{+}.*

In the case of the NK staining panel, cells were stained with BV421-rat IgG2bk anti-mouse CD3, PE-rat IgG2ak anti-mouse NKp46 and APC-armenian hamster IgG anti-mouse CD69 antibodies,

and the corresponding isotype control antibody APC-armenian hamster IgG (*Biolegend*). The NK population was defined as $CD3^-$ $Nkp46^+$, and CD69 expression was analyzed into this gated population (**Figure ES4**).

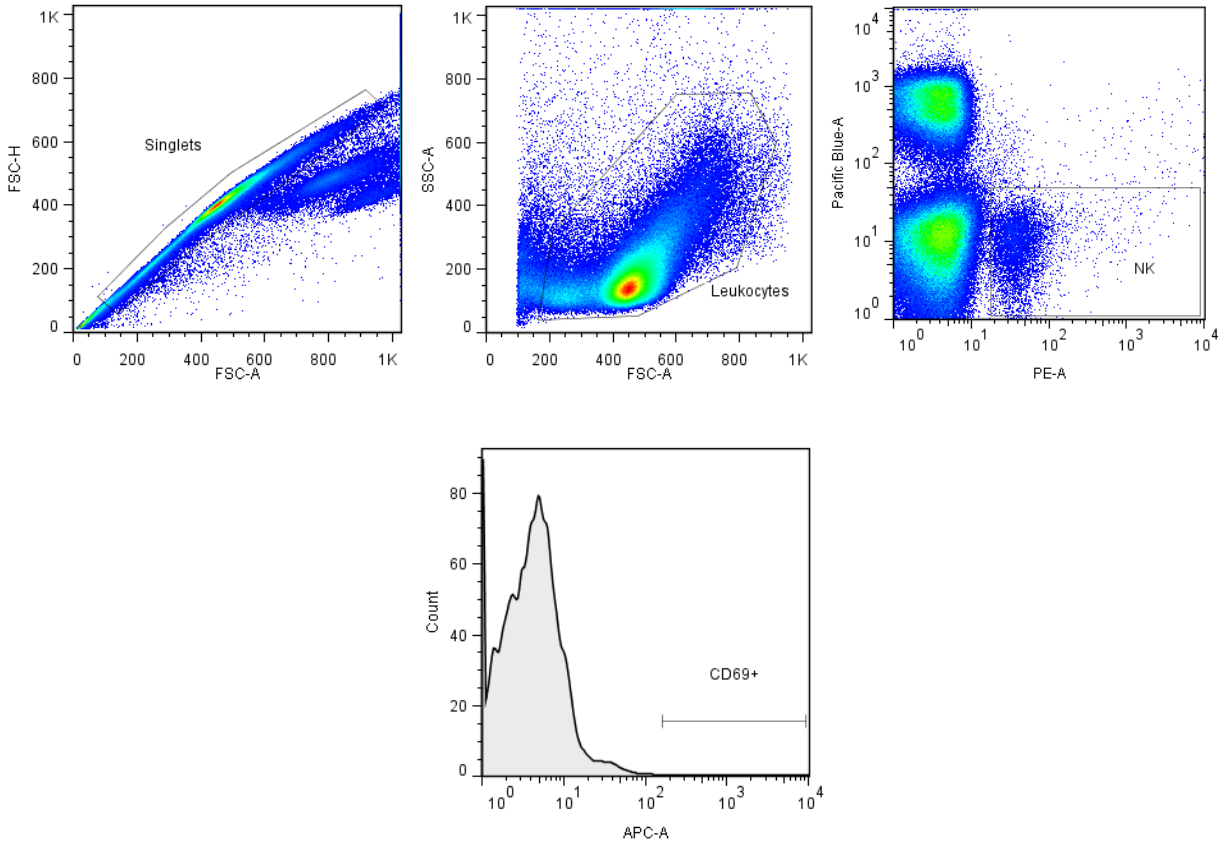

Figure ES4. *Gating strategy followed in innate immune response assays. The expression of CD69 was analyzed in a population of natural killer cells phenotypically defined as* $CD3^-$ $Nkp46^+$.

ES13. Assessing adaptive immune responses *in vivo*.

C57BL/6J mice (6-8 weeks old) were injected subcutaneously in both flanks (100 µL/flank). Mice were immunized twice with a two weeks time lapse with 5 µg OVA/mouse, 3.8 µg Poly(I:C)/mouse, 0.5 µg imiquimod/mouse and 12.1 µg/mouse ZnSPION. Blood extractions

were carried out by facial vein puncture at different timepoints (pre- and post- injection), and serum was analyzed for the presence of anti-OVA IgG antibodies by standard indirect ELISA.

Three weeks after the last immunization, mice were sacrificed by cervical dislocation and splenocytes and lymphocytes from inguinal lymph nodes and spleen were extracted as described before. SIINFEKL-specific $CD8^+$ T cells were analyzed in blood, spleen and lymph nodes. $1x10^6$ cells were stained with FITC-rat IgG2ak anti-mouse CD8 and APC-rat IgG2bk anti-mouse CD3 antibodies (*Biolegend*) to define the $CD3^+$ $CD8^+$ T cell population, specifically excluding $CD3^+$ $CD4^+$ cells. The percentage of SIINFEKL-specific cells was analyzed in the $CD3^+$ $CD8^+$ double positive population (**Figure ES5**), using PE-labeled anti-H-$2k^b$-$OVA_{257-264}$ (*Immudex*). Data are presented as an average of 5 mice per group of immunization, analyzed individually.

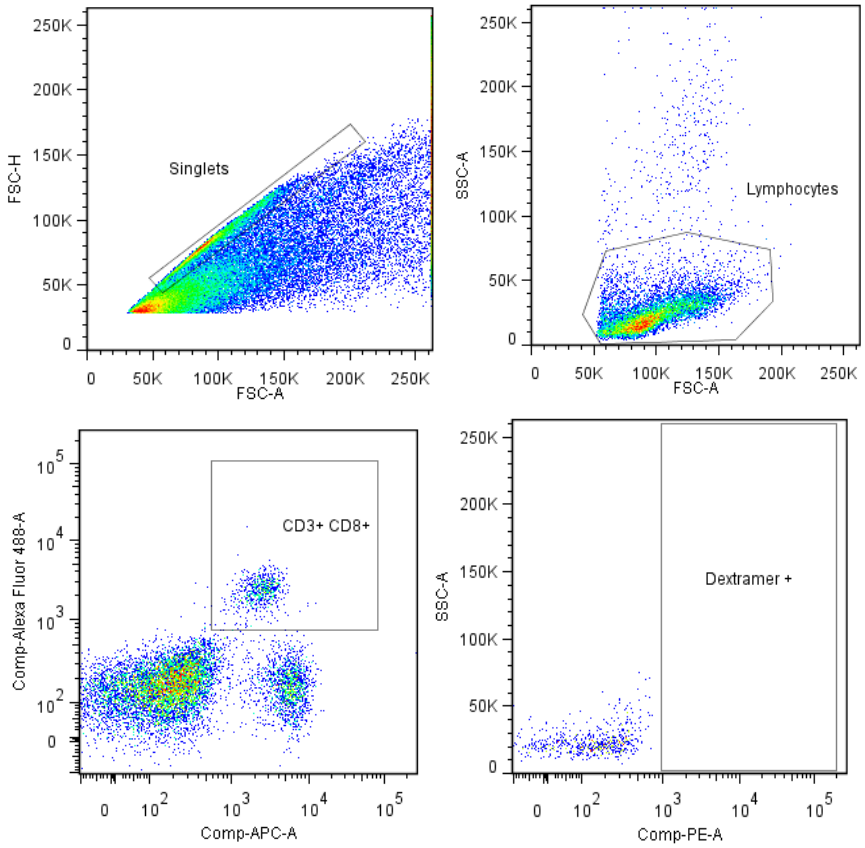

Figure ES5. *Gating strategy followed in the adaptive immune response assays. The percentage of SIINFEKL-specific $CD8^+$ T* cells *in the blood, spleen and inguinal lymph nodes of immunized mice was analyzed in a population of $CD3^+$ $CD8^+$ T lymphocytes.*

ES14. Tumor challenge *in vivo* functional studies.

C57BL/6J mice (6-8 weeks old) were immunized via subcutaneous injection on the flanks (100 μL/flank), before (prophylactic setting) or after (therapeutic setting) challenge with $3x10^5$ B16F10(OVA) tumor cells resuspended in 100 μL of PBS. Mycoplasma test (*Lonza*) was carried out prior to injection to ensure that cells were free of contamination.

In the prophylactic approach, male mice were immunized twice with a two weeks interval between both injections with 5 μg/mouse of OVA, 45.7 μg/mouse of SPION, 3.5 μg/mouse of Poly(I:C), 1.3 μg/mouse of imiquimod and 6.1 μg/mouse of ZnSPION (ZnSPION pIC-R) or with 5 μg/mouse of OVA, 45.7 μg of SPION, 10 μg/mouse of Poly(I:C), 2.3 μg/mouse of imiquimod and 12 μg of ZnSPION-DOTAP (ZnSPION-DOTAP pIC-R). Tumor cells were implanted one week after the last immunization. Blood extraction was carried out weekly to analyze the frequency of SIINFEKL-specific $CD8^+$ T cells, following the same procedure described for the adaptive immune response assays. Tumors were measured every two to three days with a digital caliper until day 31 after tumor inoculation, and volumes (V) were calculated as V (mm^3) = [(short diameter)^2 x (long diameter)]/2. Mice were considered tumor-free until dermal lesions were visible or palpable. For survival rate evaluation, mice were kept until sacrifice was necessary once the tumor reached a diameter of ≥ 15 mm or when tumor necrosis or ulceration signs appeared, according to legal requirements. In the case of mice surviving with no tumor or no signs of debilitating sickness, the experiment was ended 57 days after tumor inoculation.

In the case of prophylactic assays carried out in female mice, they were immunized twice with a two weeks interval between both injections with 5 μg/mouse of OVA, 56.6 μg/mouse of SPION, 8 μg/mouse of Poly(I:C), 2.5 μg/mouse of imiquimod and 10.1 μg/mouse of ZnSPION (ZnSPION pIC-R) or with 5 μg/mouse of OVA, 56.6 μg of SPION, 12 μg/mouse of Poly(I:C), 3.6 μg/mouse of imiquimod and 20.9 μg of SPION (SPION pIC-R). 63 days after the first tumor challenge, healthy mice were s.c. re-challenged with $3x10^5$ B16F10(OVA) cells. As a control, a group of non-inmunized mice of the same sex and age were challenged with tumor cells in parallel. Tumor volume and survival rates measurements were carried out as described above. Survivor mice were sacrificed 108 days after the first tumor inoculation and the spleen and inguinal lymph nodes were extracted to analyze the immunological memory response developed.

Splenocytes and lymphocytes primary cell cultures were established as described above and divided into two groups for the characterization of the magnitude and quality of the memory response. In the first case, $1x10^6$ cells were stained with PE/Cy7-rat IgG2ak anti-mouse CD8 and BV421-rat IgG2bk anti-mouse CD3 antibodies (*Biolegend*) to define the $CD3^+$ $CD8^+$ T cell population. The T central memory population (Tcm) is defined as $CD62L^+CD44^+$ while the T effector memory population (Tem) is $CD62L^-CD44^+$. The percentage of SIINFEKL-specific cells was analyzed (**Figure ES6**) in both populations (Tem and Tcm), using PE-labeled anti-H-$2k^b$-$OVA_{257-264}$ (*Immudex*). Data are presented as an average of all the survivor mice in each group of immunization, analyzed individually. In order to assess the quality of the memory response, the production of the key intracellular cytokines TNFα, IFNγ and the degranulation marker CD107a was measured (**Figure ES7**) by intracellular FACS (icFACS). In this case, $1x10^6$ cells were stained with FITC-rat IgG2ak anti-mouse CD8 and BV421-rat IgG2bk anti-mouse CD3 antibodies (*Biolegend*) to define the $CD3^+$ $CD8^+$ T cell population. TNFα, IFNγ and CD107a were stained with PE/Cy7-rat IgG1k anti-mouse TNFα, APC-rat IgG1k anti-mouse IFNγ and PE-rat IgG1ak anti-mouse CD107a (LAMP-1) (*Biolegend*), respectively.

The *in vivo* synergistic immunostimulatory activity of the combined TLR agonists Poly(I:C) and imiquimod was demonstrated in female mice following the same procedure described for the prophylactic immunization assays. In this case, mice were immunized twice with 5 μg/mouse of OVA, 4 μg/mouse of Poly(I:C) and 2 μg/mouse of imiquimod, either individually or in combination. Tumor volume and survival rates measurements were monitored as described above for 48 days.

In the therapeutic approach, female mice were immunized three times on days 4, 7 and 11 after tumor implantation with 5 μg/mouse of OVA, 27.1 μg/mouse of SPION, 8 μg/mouse of Poly(I:C), 2.3 μg/mouse of imiquimod and 10.1 μg/mouse of ZnSPION (ZnSPION pIC-R) or with 5 μg/mouse of OVA, 12 μg/mouse of Poly(I:C), 2.4 μg/mouse of imiquimod and 17.1 μg/mouse of ZnSPION-DOTAP (ZnSPION-DOTAP pIC-R). For tumor volume measurements and survival rate assessment, we proceeded as described in the prophylactic setting.

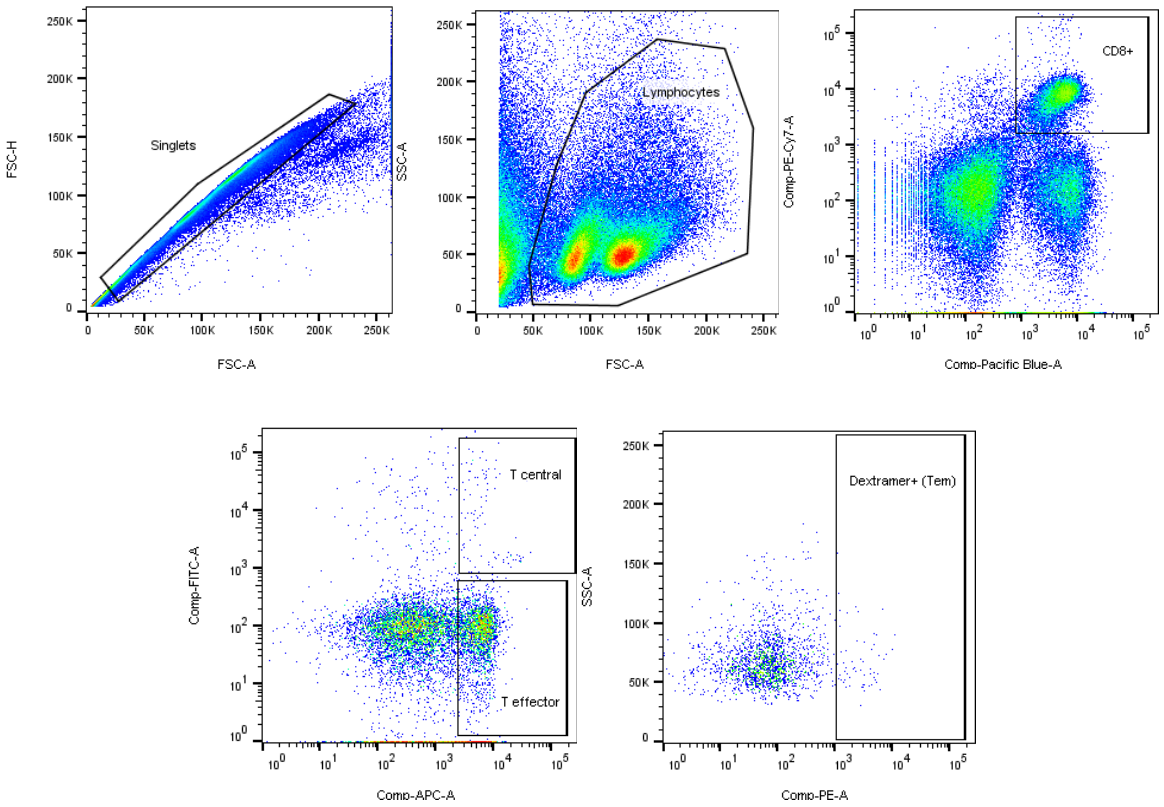

Figure ES6. *Gating strategy followed for the analysis of the magnitude of the immunological memory response generated at the end of the prophylactic immunization assay. The size of the T central (Tcm; CD62L$^+$CD44$^+$) and T effector (Tem; CD62L$^-$CD44$^+$) memory populations was determined in a population of CD3$^+$ CD8$^+$ T lymphocytes. The percentage of SIINFEKL-specific T-*cells *in the spleen and inguinal lymph nodes of immunized mice was analyzed in the population of CD3$^+$ CD8$^+$ Tem lymphocytes.*

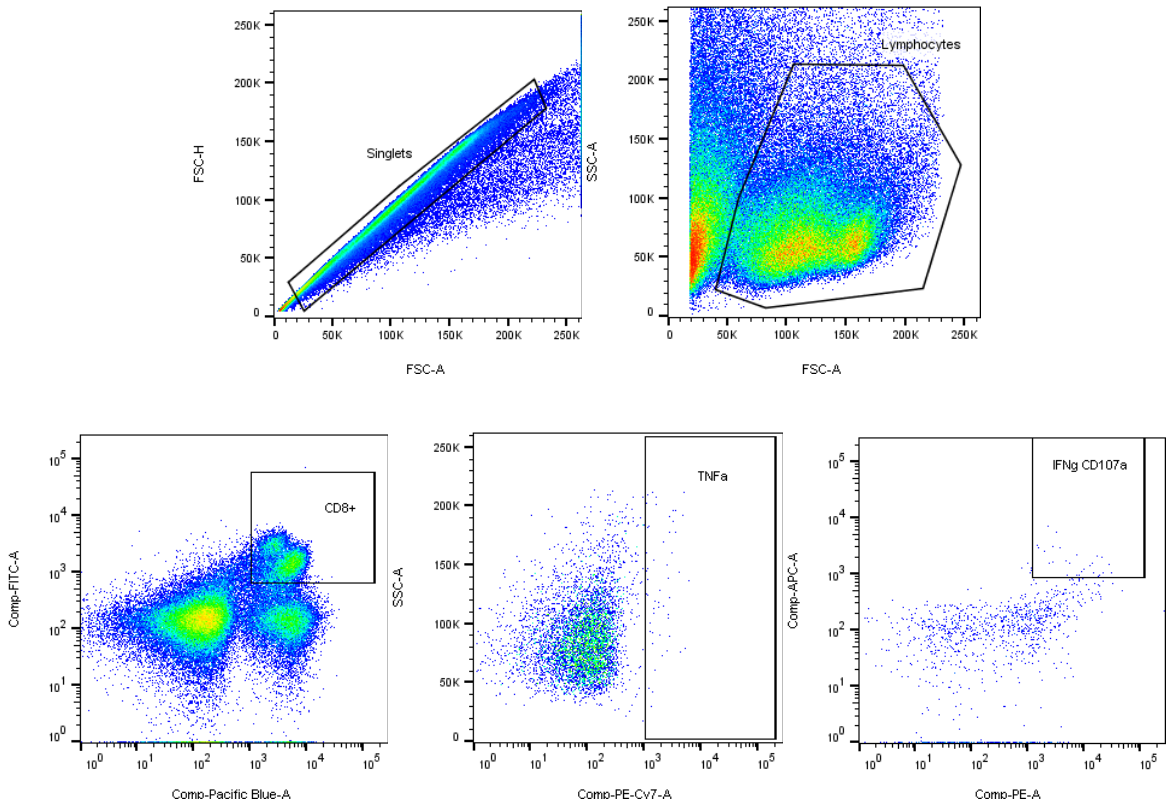

Figure ES7. *Gating strategy followed for the analysis of the quality of the immunological memory response generated at the end of the prophylactic immunization assay. The intracellular production of the key cytokines TNFα, IFNγ and the degranulation marker CD107a was analyzed by intracellular FACS in the population of $CD3^+$ $CD8^+$ T lymphocytes.*

ES15. *In vivo* prophylactic immunization assays with modified B16F10(OVA) cell lines.

Modified B16F10(OVA) with knock-down expression of PD-L1 (B16F10(OVA) C-C PD-L1) were obtained as result of a collaboration with the group of Dr. David Escors from Navarrabiomed (Pamplona, Spain). Briefly, lentiviral particles for silencing the expression of PD-L1 were produced in 293T cells. Cell culture supernatants were harvested, filtered through 0.45 µm filter and ultracentrifuged for lentivectors purification. Lentiviral particles were titrated and used to transduce B16F10(OVA) cells. Knockdown cells were selected by antibiotic pressure with increasing concentrations of puromycin.

Similarly to the prophylactic immunization assays described above, C57BL/6J female mice (6-8 weeks old) were immunized via subcutaneous injection on the flanks (100 µL/flank), before a tumor challenge with $3x10^5$ B16F10(OVA) C-C PD-L1 cells resuspended in 100 µL of PBS. Mycoplasma test (*Lonza*) was carried out prior to injection to ensure that cells were free of contamination.

Mice were immunized twice with a two weeks interval between both injections with 5 µg/mouse of OVA, 56.6 µg/mouse of SPION, 8 µg/mouse of Poly(I:C), 1.1 µg/mouse of imiquimod and 8.9 µg/mouse of ZnSPION (ZnSPION-DOTAP pIC-R). Tumor cells were implanted one week after the last immunization. 35 days after the first tumor inoculation, a contralateral tumor re-challenge with 1.5×10^6 B16F10(OVA) C-C PD-L1 cells/mouse was carried out. Tumor volume and survival rates measurements were carried out as usual for 108 days.